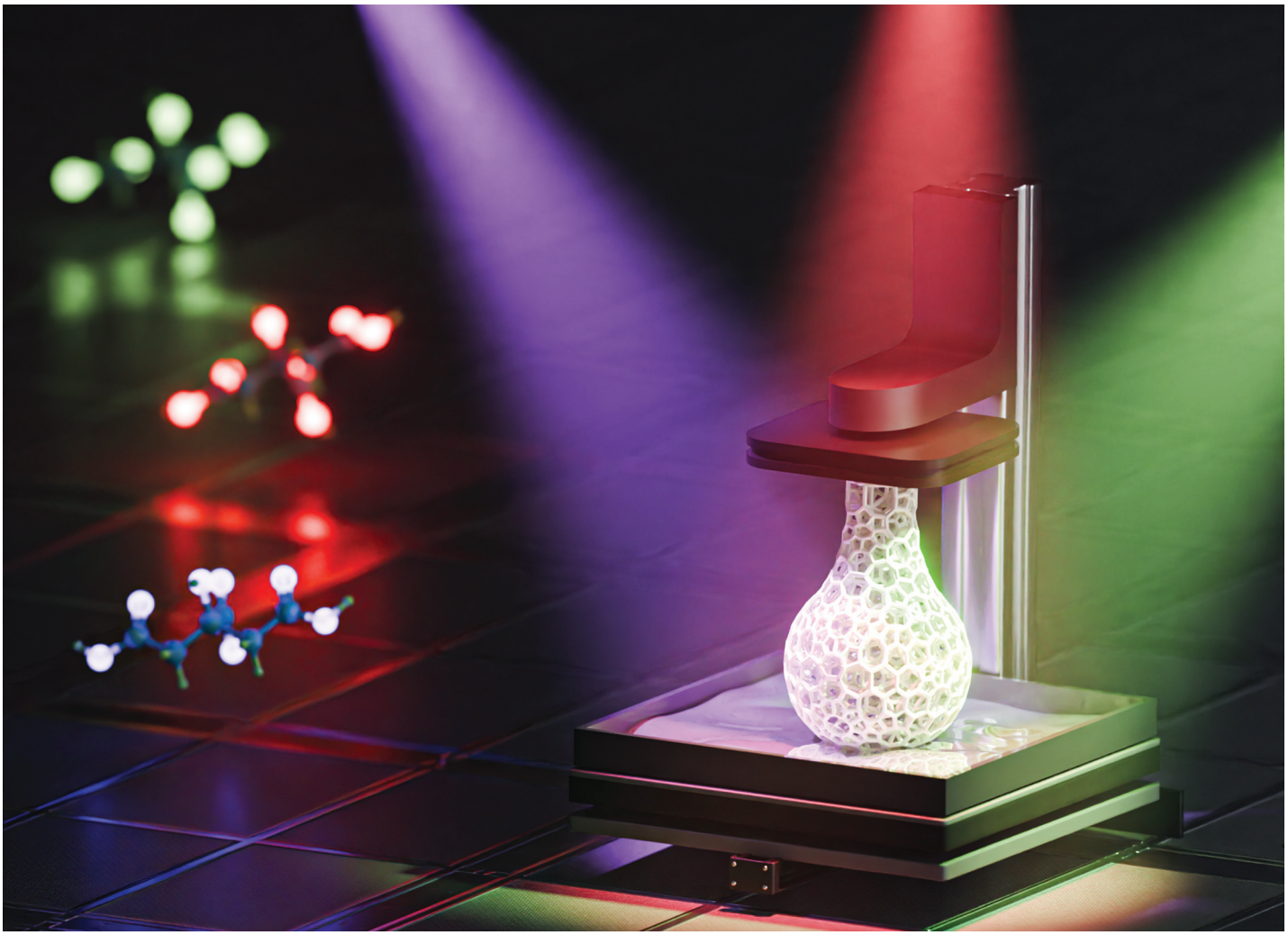

Highlighting perspectives from early-career researchers from around the world, led by Professor Max A. Saccone, Department of Mechanical Engineering, University of Colorado Boulder, Boulder, CO, USA and Abhishek Dhand, Department of Bioengineering, University of Pennsylvania, Philadelphia, PA, USA.

Advances in vat photopolymerization: early-career researchers shine light on a path forward

Early-career researchers from around the world summarize recent developments and present visions for the future of vat photopolymerization 3D printing.

Image reproduced by permission of Max A. Saccone from *RSC Appl. Polym.*, 2025, **3**, 574.

As featured in:

See Saccone & Dhand *et al.*, *RSC Appl. Polym.*, 2025, **3**, 574.

ROYAL SOCIETY OF CHEMISTRY

rsc.li/RSCApplPolym

Registered charity number: 207890

RSC Applied Polymers

ROYAL SOCIETY OF CHEMISTRY

PERSPECTIVE

View Article Online
View Journal | View Issue

Cite this: *RSC Appl. Polym.*, 2025, **3**, 574

Advances in vat photopolymerization: early-career researchers shine light on a path forward

Abhishek P. Dhand,*[a] Ren H. Bean,[b] Viviane Chiaradia,[c] Alex J. Commisso,[b] Dalia Dranseike,[d] Hayden E. Fowler,[b] Julia M. Fraser,[e] Holden Howard,[f] Takashi Kaneko,[g] Ji-Won Kim,[h] Jason M. Kronenfeld,[i] Keldy S. Mason,[j] Connor J. O'Dea,[j] Fred Pashley-Johnson,[k,l] Dominique H. Porcincula,[f] Maddison I. Segal,[m] Siwei Yu[n] and Max A. Saccone*[o,p]

Vat photopolymerization (VP) has emerged as a promising additive manufacturing technique to allow rapid light-based fabrication of 3D objects from a liquid resin. Research in the field of vat photopolymerization spans across multiple disciplines from engineering and materials science to applied chemistry and physics. This perspective brings together early-career researchers from various disciplines in academia and national laboratories around the world to summarize the most recent advancements with special emphasis on the research highlighted as part of the Gordon Research Conference (GRC) 2024 meeting on Additive Manufacturing of Soft Materials. We provide an outlook on next-generation polymer processing methods from synthesis of novel materials to multimodality manufacturing and performance engineering. Further, this article combines the ideas of many of these junior researchers to present a vision for the future of the field by highlighting the challenges and opportunities that lie ahead.

Received 19th January 2025,
Accepted 4th March 2025

DOI: 10.1039/d5lp00010f

rsc.li/rscapplpolym

1. Introduction

Vat photopolymerization (VP) is a widely used additive manufacturing (AM) technique which enables three-dimensional (3D) fabrication of objects through spatially controlled light-initiated crosslinking of a liquid photoresin (Fig. 1A).[1,2] Process workflow for VP involves an input in the form of a computer aided design (CAD) object which is then converted into 2D images or a scan path to be projected using the printer light modality. When compared to other AM methods such as direct-ink writing (DIW) or inkjet printing, VP methods exhibit higher resolution and faster printing speeds due to a layer-by-layer fabrication approach instead of linear filament or droplet deposition.[3] Throughout this article, we use the term 'resin' to denote the photoreactive solution containing monomer/macromer along with photo-additives (*e.g.*, initiators, absorbers) and the term 'crosslink' to describe the solidification of the liquid resin (*i.e.*, the polymerization of reactive monomers into a polymer network or the reaction of functionalized polymers directly into networks).

Developments in light delivery techniques, printer hardware engineering, and materials design over the past few decades have led to VP being widely adopted in both academia and industry, with techniques like stereolithography (SLA) and digital light processing (DLP) gaining tremendous attention. SLA and multi-photon lithography (MPL) utilize a laser that is raster scanned along or within the vat volume to crosslink a resin into a 3D object in a point-by-point manner.[4] Multi-

[a]*Department of Bioengineering, University of Pennsylvania, Philadelphia, PA, USA. E-mail: adhand@seas.upenn.edu*
[b]*Sandia National Laboratories, Albuquerque, NM, USA*
[c]*Department of Chemistry, RCSI University of Medicine and Health Sciences, Dublin, Ireland*
[d]*Macromolecular Engineering Laboratory, Department of Mechanical and Process Engineering, ETH Zurich, Zurich, Switzerland*
[e]*Department of Chemistry, University of Wisconsin-Madison, Madison, WI, USA*
[f]*Materials Engineering Division, Lawrence Livermore National Laboratory, USA*
[g]*Department of Chemistry and Biochemistry, University of California, Santa Barbara, CA, USA*
[h]*Department of Chemical Engineering, Kyungpook National University, Daegu, Republic of Korea*
[i]*Department of Chemistry, Stanford University, Stanford, CA, USA*
[j]*Department of Chemistry, The University of Texas at Austin, Austin, TX, USA*
[k]*School of Chemistry and Physics & Centre for Materials Science, Queensland University of Technology (QUT), Brisbane, QLD, Australia*
[l]*Centre of Macromolecular Chemistry (CMaC), Department of Organic and Macromolecular Chemistry, Faculty of Sciences, Ghent University, Ghent, Belgium*
[m]*Thomas Lord Department of Mechanical Engineering & Material Science, Duke University, Durham, NC, USA*
[n]*Department of Chemistry, University of Washington, Seattle, WA, USA*
[o]*Department of Chemical Engineering, Stanford University, Stanford, CA, USA. E-mail: max.saccone@colorado.edu*
[p]*Paul M. Rady Department of Mechanical Engineering, University of Colorado Boulder, Boulder, CO, USA*

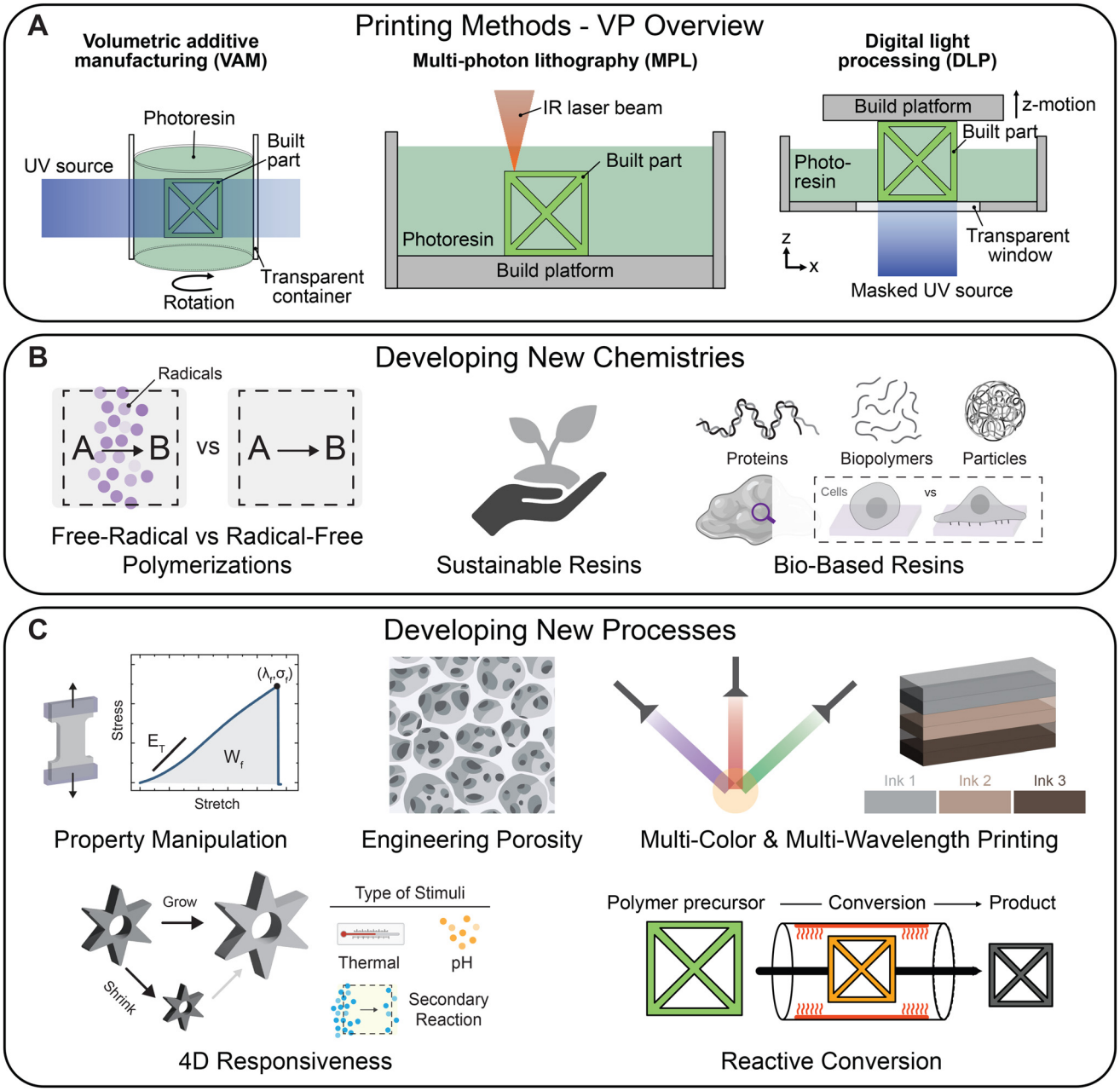

Fig. 1 Overview of vat photopolymerization (VP) to enable fabrication of functional materials. (A) Schematic representation of lithography-based 3D printing methods: volumetric additive manufacturing (VAM), multi-photon lithography (MPL), and digital light processing (DLP). (B) Schematic outline of key chemistries including development of radical-free reactions, resins derived from sustainable feedstocks, and bio-based formulations to engineer living materials. (C) Schematic outline of key single or multi-color/multi-material printing processes including development of methods to tune mechanical properties, introduce porosity, engineer dynamic responsiveness, or enable reactive conversion of 3D printed objects.

photon lithography can achieve much smaller feature sizes at sub-100 nm resolution albeit at the cost of slow speed of fabrication.[5] The three commonly reported mechanisms for two-photon absorption in direct laser writing (DLW) include upconversion luminescence, two-step absorption, and triplet–triplet annihilation.[6] Theoretically, these modalities can lead to printed features much smaller than the wavelength of light used, but in reality, the resolution is limited by optical diffraction. This diffraction barrier can be overcome with processes inspired by stimulated-emission-depletion (STED) microscopy wherein excited photoinitiator molecules outside the laser focus are brought to the ground state by a second, different color laser beam, resulting in finer resolution.[7]

DLP involves top-down or bottom-up planar light projection of sequential 2D sliced images within a vat for stepwise fabrication of 3D objects onto a motorized build platform.[8] Each digitally displayed image contains an array of square pixels that crosslink the resin locally to form single-layer 3D rec-

tangular bricks called voxels. Unlike SLA, the print time for DLP printing is solely dependent on the height (depth) and exposure time for each layer, as the entire layer is cured simultaneously. However, the resolution in the case of DLP is often restricted by the pixel size (~1 to 100 μm) of the digital micromirror device (DMD) array. In contrast to sequential light projection, 3D objects can be rapidly (>50 cm h^{-1}) fabricated *via* continuous liquid interface production (CLIP)[9] or high area rapid printing (HARP)[10] which utilize non-polymerizable interfaces based on oxygen inhibition or circulating fluorinated oils, respectively, to reduce adhesion force and permit continual replenishing of fresh uncured resin. Continuous build platform motion also eliminates the staircasing effect that stems from layer-by-layer fabrication. Another layerless fabrication technique, volumetric additive manufacturing (VAM), enables volumetric photopolymerization for example by projecting sliced images into a synchronized, rotating vat from all angles to allow accumulation of a 3D light dose required for gelation.[11,12] In addition to the high speed of fabrication, the unique ability of VAM to support overprinting (*i.e.*, cross-linking material around a complex, preexisting 3D structure) is highly advantageous when combination with other fabrication techniques (*e.g.*, DIW or melt-electrowriting) is desired.[13–15] Significant recent emphasis has been placed on enhancing VP printing rates and resolution through dual color xolography[16] or acoustically modulated, dynamic interface printing[17] for fabrication of high resolution, centimeter scale constructs in tens of seconds. The wide array of fabrication strategies and materials combined with the accessibility of DLP or VAM techniques has led to their applications across numerous fields, from biomedical devices and energy materials to sporting equipment, aviation and automotive industries.

This article aims to combine ideas from early-career researchers through the lens of the Gordon Research Seminar (GRS) and Gordon Research Conference (GRC) 2024 meeting on Additive Manufacturing of Soft Materials. We first present a guide for resin design highlighting the present best practices for characterization discussed at the meeting. With special emphasis on manipulating reactivity, rheology, or resolution, we next highlight novel methods for reaction chemistries and processing for a broad range of materials from thermosets and thermoplastics to hydrogels, organogels, and composites (Fig. 1B and C). Finally, we address the resolution-throughput tradeoff by highlighting recent examples that enable scalable production. Importantly, we seek to highlight recent developments in vat photopolymerization for 3D printing, particularly DLP and VAM, with a goal to provide a forward-looking perspective on the challenges and opportunities that lie ahead in the field. For more comprehensive, in-depth insights on vat photopolymerization, we direct our readers to other specialized reviews.[18,19]

2. Best practices for resin design

Various design principles must be considered when formulating resins for VP. These include but are not limited to the type of polymerization reaction, choice of reactive species (*i.e.*, type and concentration), viscosity, optical properties of the resin (*i.e.*, type and concentration of photoinitiator, photoinhibitor or photoabsorber) and printer specifications (resolution, light intensity, wavelength and spectral bandwidth, slicing thickness, and movement speed of the build platform or vat).[3] Within the scope of VP, developing novel materials, initiation approaches, orthogonal chemistries, and technique modifications are inherently dependent on light propagation through the setup and resin medium. This has historically been described *via* the Jacobs working curve from laser-based stereolithography:

$$C_d = D_p \ln\left(\frac{E}{E_c}\right)$$

where D_p is the penetration depth into the photopolymerizable medium at which the incident intensity is reduced by $1/e$, E is the light dosage delivered to the medium, E_c is the light dosage threshold to reach gelation, and C_d is the resultant depth to which resin is cured relative to the incident plane. These working curves for resins can be obtained *via* measurements of cure depths as a function of irradiant energy using contact (*e.g.*, atomic force microscopy, AFM or digital calipers) or non-contact (*e.g.*, laser scanning confocal microscopy or scanning electron microscopy) methods. While the Jacobs equation has been an essential cornerstone of the VP field, the methods for measuring intrinsic resin properties (D_p and C_d) vary across laboratories resulting in vast variation and thus lack of translated repeatability.[20] These discrepancies can be attributed to non-linearities in the Jacobs model and sources of error in measurement approach (*in situ vs. ex situ*). It is critical to note that the spectral bandwidth of the light source can also contribute an inner filter effect that causes working curves to deviate from linearity; light source characterization and calibration are highly recommended.[20–22] Further, when designing a novel resin for vat photopolymerization, it is important to consider the performance-processability tradeoff. For instance, introduction of UV-absorbing agents may decrease D_p and thus increase part resolution, but may negatively impact the desired material properties, for instance mechanical strength or cytocompatibility.

Although there is a need for standardization of reported parameters, instrumentation setup, and subsequent augmentations, here we outline a preliminary checklist for characterization:

1. Resin formulation: Researchers should report the relative percentage of all components included and the protocol for mixing components (if any) as well as storage conditions. Additionally, viscosity of the resin should be reported (including the specific shear rate used during the measurement and details of the instrumentation and conditions utilized).

2. Light source wavelength and intensity: Researchers should report details about the light source (namely, wavelength, spectral bandwidth, and intensity) utilized while printing and while constructing working curves. If applicable, the

associated variation in intensity observed over time and along the entire build area should also be reported.

3. Working curve: Researchers should note the method of curing (*e.g.* cured on glass slide, bridges cured), method of measuring (*e.g.* digital calipers, profilometer, or microscopy-based), and report values for D_p and E_c along with associated error. If possible, include the raw data on an open data repository to make it accessible to other readers.

4. Minimum feature size: Researchers should report the minimum feature size obtained on a printed object. This should be done in both 'as printed' as well as 'swelled/shrunken state' (if the shape changes significantly after printing). Minimum feature size can include measurements of a single voxel or a smallest resolvable feature.

5. Additional suggested parameters to report: It is recommended to report a spectral absorbance profile (optical density) of the resin formulation. Researchers should consider reporting other curing parameters specific to the printer used such as exposure time for base and body layers, post-exposure delay, stage velocity, stage acceleration, acquiescence time (pre-exposure, post-move), rate of rotation, layer step size, and gain relative to working curve.

3. Developing new chemistries for VP

Monomers or macromers with acrylate, methacrylate, acrylamide, or methacrylamide groups are often used in photocurable resins because they can quickly undergo radical polymerization to form crosslinked networks.[23] While this is a common and effective method for crosslinking, the use of radical polymerization crosslinking imparts many issues including uncontrolled network formation, potential for part shrinkage, and formation of non-degradable C–C bonds in the polymer backbone.[24] Here, we outline key advances at the forefront of developing novel chemistries and material-driven approaches for VP.

Moving beyond chain-growth radical polymerizations

Although the formation of polymer networks *via* VP most commonly relies on chain-growth radical polymerization, these reactions and residual uncured monomers can cause damage to biological systems (*e.g.*, cells and proteins), affect long-term ambient stability (*e.g.*, aging), and restrict the breadth of material properties. Therefore, it is desirable to develop alternative VP strategies that are more compatible and efficient than radical chemistries.[25,26]

One such alternative is the family of radical-mediated photo-click reactions (*e.g.*, thiol–ene), which can result in high selectivity, high yields, and versatility.[27,28] For instance, tunable mechanical properties can be realized by changing the molar ratio of thiols to alkenes to adjust the extent of crosslinking (Fig. 2A).[29] Selectivity of thiol–ene reactions allows for functional groups of interest to be readily incorporated into polymers or crosslinkers. While photo-click reactions have potential to improve network uniformity, issues with controlling network topology can lead to defects through backbiting or formation of dangling chains or loops; such defects can weaken the mechanical properties of the printed materials.[30] Current experimental methods like nuclear magnetic resonance (NMR) or Fourier transform infrared (FT-IR) spectroscopy can determine the extent of crosslinking by tracking the conversion of reactive groups but cannot reliably distinguish between inter- and intramolecular crosslinking. Modeling efforts to better understand deviations from ideal network behavior[31] can enable photochemical reactions (*i.e.*, chain-, step-, or mixed-mode) to be leveraged to control network topology, allowing access to a broader range of mechanical properties.[32]

Another promising alternative set of techniques is the family of radical-free polymerizations. One such strategy, ring-opening metathesis polymerization (ROMP), polymerizes cyclic olefins, typically using transition metal catalysts, and can allow for precise control over polymer characteristics, including molecular weight, tacticity, and stereochemistry, which are more difficult to tune using radical polymerizations.[33] While industrial applications often rely on initiation methods like heat and redox reactions, photoinitiated ring-opening metathesis polymerization (photoROMP) processes are promising because of their energy efficiency and spatiotemporal control over catalyst activity.[34] The progress in photoactivation systems has been driven by the ability to control latent ruthenium (Ru) metathesis catalysts with light through the incorporation of photosensitizers and coinitiators to modulate polymerization rates. Furthermore, the use of light-triggered photobase generators to deactivate polymerization has led to the development of selective dual-wavelength olefin metathesis, enabling continuous vat photopolymerization.[35] To date, photoROMP has primarily been applied to the additive manufacturing of poly(dicyclopentadiene), a high-performance thermoset known for its excellent thermal stability, mechanical properties, and chemical resistance (Fig. 2B).[36] However, other monomer and catalyst combinations remain to be explored. For instance, degradable materials fabricated *via* photoROMP highlight the sustainability potential of this technology, while the exploration of multi-material systems could further expand its applications.[37,38] Despite growing interest in developing photoROMP-based resins, several challenges must be addressed. The addition of catalysts often limits the pot life of ROMP-based resins, and the use of latent metathesis catalysts in vat photopolymerization can compromise reaction kinetics.[39,40] To improve additive manufacturing systems, a deeper understanding of indirect initiation mechanisms involving photosensitizers and coinitiators is essential. This knowledge will facilitate the development of systems with faster production speeds that require lower light irradiance, as current implementations typically require layer exposures of >10 s and high irradiance, making them less competitive compared to established radical-based systems.[40] By overcoming these challenges, photoROMP could enable access to a broader range of material systems and properties, as well as facilitate the exploration of other vat photopolymerization techniques, such as VAM.[41] Additionally, integrating other

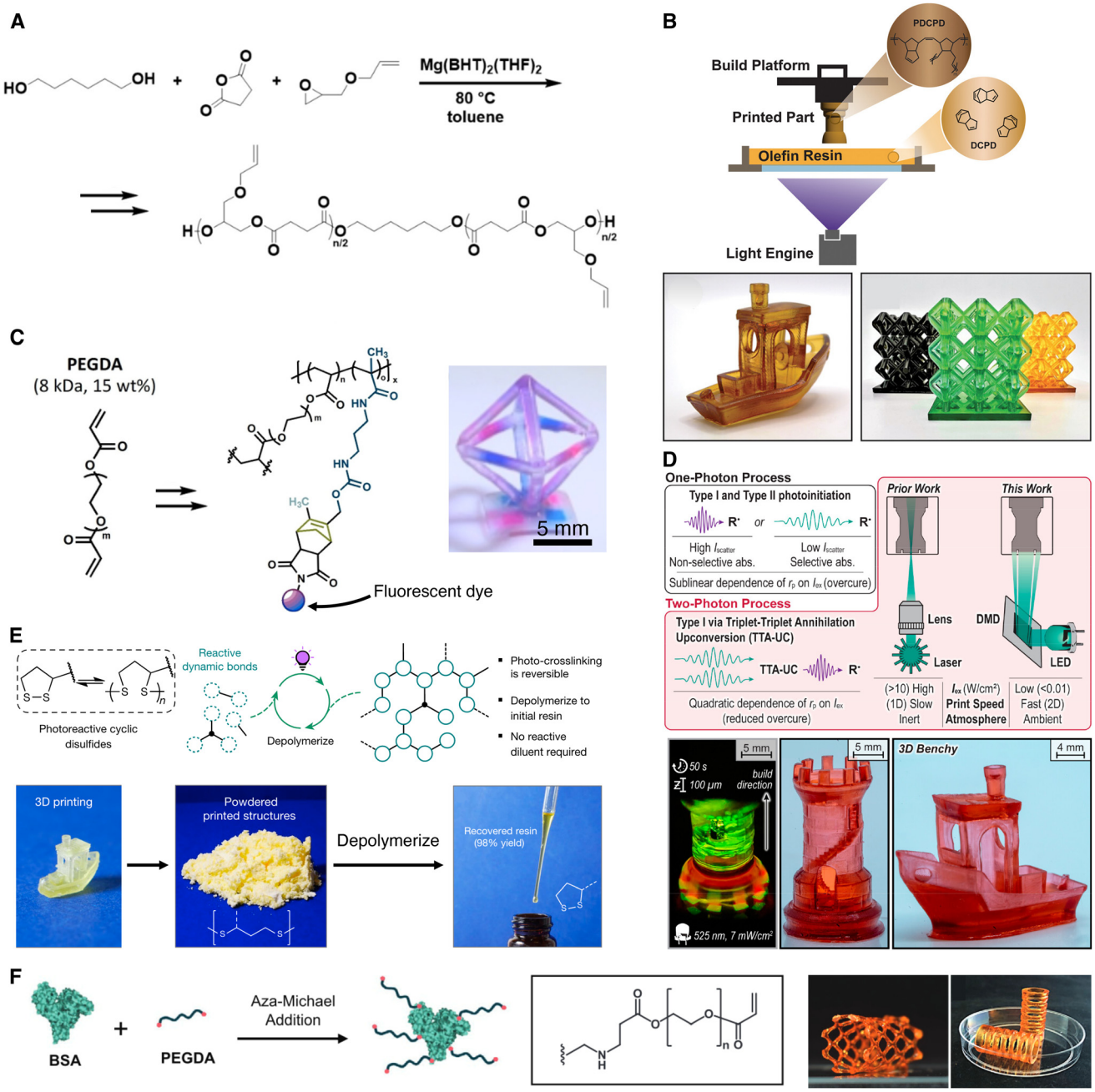

Fig. 2 Development of new chemistries for VP of functional materials. (A) Synthesis of poly(allyl glycidyl ether succinate) (PAGES), a degradable polyester, *via* ring opening copolymerization enables DLP printing with the addition of thiol crosslinkers to enable thiol–ene click reactions. (B) Photoinitiated ring-opening metathesis polymerization of dicyclopentadiene (DCPD) enables 3D printing with olefin resins. (C) Synthesis of cyclopentadienone-norbornadiene (CPD-NBD) adducts for radical-free Diels–Alder photopatterning and incorporation into PEGDA-based 3D printing resins. (D) Triplet–triplet annihilation upconversion (TTA-UC) enables DLP printing with green light at low radiant exposure (<10 mW cm^{-2}). (E) Incorporation of dynamic disulfide bonds enables closed-loop recycling of 3D printing resins derived from sustainable sources. (F) Incorporation of bovine serum albumin (BSA) protein-based materials into 3D printing resins *via* aza-Michael addition enables enzymatic degradation of printed parts. Adapted with permission from (A),[29] (B),[34] (C),[54] (D),[59] (E),[80] (F).[94]

photoactivated methods, including photophysical[42–44] and metal-free systems,[45] presents exciting opportunities for future research.[26–29]

Furthermore, there has been a growing interest in leveraging dynamic covalent chemistries (*e.g.*, disulfides, boronic ester cycloaddition, or urethane transamination) for VP.[46] Of note, Diels–Alder (DA) cycloadditions are highly efficient dynamic covalent click reactions and are widely used in organic synthesis, materials science, and bioconjugation.[47] Unlike other common click chemistries that rely on toxic

copper catalysts, additives, or radicals,[48] DA cycloadditions offer high efficiency, variable reaction rates, functional group tolerance, and additive-free methods while maintaining biocompatibility. Inspired by the high reactivity of cyclopentadiene and its advantages in macromolecular click reactions, the Read de Alaniz group has reported the development of cyclopentadienone with maleimide or norbornadiene DA adducts[49–53] and their application to post-functionalization of 3D-printed hydrogels (Fig. 2C).[54] These adducts work as photocages of cyclopentadiene that enable efficient photo-induced bioconjugation and control of polymer click reactions without the need for radicals. For instance, after printing, 3D hydrogels can be photo-patterned using masked irradiation at 365 nm light, enabling high resolution spatial functionalization of various biological cues. This highlights the versatility and user-friendly nature of the patterning platform for creating complex hydrogel applications in biomedical fields, particularly in tissue engineering.

In VP, the majority of photoinitiators (known as Type I initiators) require ultraviolet (UV) light for efficient radical generation *via* homolytic bond cleavage. However, visible light offers several advantages such as improved safety, increased energy efficiency with LED sources, selective absorbance, and reduced scattering, which together can enhance object resolution and broaden the range of accessible materials.[55,56] A variety of techniques have been investigated to initiate radical polymerizations with visible light by either red-shifting Type I initiators *via* chemical modifications or developing photosystems that utilize photoredox catalysis to generate radicals (known as Type II initiators). Resins using a Type II mechanism require a combination of a photosensitizer and charged co-initiator salts (*i.e.* electron donor and acceptor) that are often chemically labile even under dark conditions which limits the pot-life and scalability of such resins. Triplet–triplet-annihilation upconversion (TTA-UC) is an emerging technique for visible light initiated photopolymerization through the indirect activation of a Type I photoinitiator.[57,58] TTA-UC enables generation of high energy light (*e.g.* green-to-violet, red-to-blue) within a resin by converting two photons of low energy through absorption by a photosensitizer. As this mechanism operates solely through energy transfer, it obviates reactive intermediates (*i.e.* charged radical species) which can cause undesirable side reactions and catalyst degradation. Further, the activation of a Type I initiator *via* TTA-UC confers a superlinear dependence of the polymerization rate on light irradiance which helps to mitigate overcure from low-irradiance scattered or transmitted light (Fig. 2D). Although triplet upconversion is highly oxygen sensitive, polymerization under ambient conditions is possible, aided by the inclusion of oxygen scavengers (*e.g.* triphenylphosphine, ascorbic acid, or thiols).[59] Assisted by the technological advancements in 3D printing hardware (*e.g.* mechanical design, optics, and excitation sources), the synthesis of new photosensitizer/annihilator combinations and resin optimization will increase the scope of usable wavelengths, light irradiances, and resin compositions.

Moving towards reprocessable networks

Although VP has been largely limited to thermosets, thermoplastics offer reprocessability and often achieve impressive mechanical properties not realized among intractable thermosets. However, VP of thermoplastics, specifically DLP, is difficult to achieve due to the constraint requiring the solid photopolymerized polymer to separate from the remaining liquid in the resin bath. The absence of cross-linking yields linear polymers that are more likely to dissolve or disperse within the monomer resin. This challenge requires careful resin design to balance photopolymerization kinetics, polymer glass transition temperature (T_g), and/or crystallization kinetics to prevent undesirable polymer dissolution.[60,61] Particularly, layer wise printing of semi-crystalline polymers *via* DLP adds additional challenges in interlayer adhesion when the polymer chains do not span the crystalline domains between each printed layer. To this end, strategies such as addition–fragmentation chain transfer (AFCT) chemistry have been implemented to improve printability by rearranging polymer connectivity and enhancing interlayer adhesion.[62] Further, the processing of thermoplastics *via* DLP often requires polymers with high Tg or semi-crystallinity, thereby limiting the final material properties to stiff and brittle. However, the material properties can be expanded through careful design of double network thermoplastics that yield soft and compliant structures.[63] The future potential of high resolution thermoplastic DLP is exciting, but challenges remain to make it relevant in commercial applications. Beyond conventional radical polymerization, new strategies using RAFT (reversible addition–fragmentation chain transfer)[64] and photo-ROMP hold promise for printing of olefinic thermoplastic polymers.[40] Research focusing on developing tough and elastic photopolymers combined with methods for improving both the polymerization and crystallization kinetics will further enhance the potential of thermoplastic processing.

Designing circular, sustainable, and bio-derived resins

The high performance of polymeric networks for a wide range of applications has spurred the growth of the photo-curable resin market; however, most commercial resins are sourced from petroleum. In alignment with global environmental concerns, it is necessary to develop sustainable alternatives for photoresins and to reconsider of the full life cycle of printed plastics, including their recyclability. Consideration of end-of-use processing has led to development of alternatives such as recyclable polythiourethane,[26] degradable photoROMP materials,[34] and reprocessable networks from cationic reversible addition–fragmentation chain-transfer polymerization (RAFT) of vinyl ethers.[65] The use of bio-based feedstocks, such as polypeptides,[66] proteins,[67–69] terpenes/terpenoids,[70] provides a greener alternative for degradable networks.

Sustainable resin design approaches making use of bio-based feedstocks have attracted increasing attention to reduce the reliance on petrochemical feedstocks. Bio-based feedstocks such as vegetable oils (including sunflower, canola, soybean,

olive, and sesame oils) have been utilized as precursors for resin design on account of their chemical versatility and wide availability.[71,72] Protein-based resins are another example of bio-sourced resins to prepare complex 3D objects. Nelson and coworkers have developed bovine serum albumin (BSA)-based bioplastics using two fabrication routes: one that utilizes aza-Michael addition of acrylate functionalities with lysines on BSA and the other uses methacrylate-modified BSA for *in situ* functionalization.[68,73] These resins can be used for DLP printing of 3D objects in a hydrogel state that can be subsequently dehydrated to form bioplastics that exhibit shape memory properties and biodegradability.[69,74]

Importantly, most reported approaches rely on (meth)acrylation and epoxidation of bio-based feedstocks, limiting the ability to form controlled network structures and rendering the materials non-degradable after crosslinking; there is a need for greener crosslinking chemistries in addition to the use of sustainable feedstocks. To that end, naturally-derived terpenes and terpenoids have been exploited as replenishable feedstocks for creating greener resins for AM. Dove and coworkers designed resins with monomers derived from myrcene, linalool, limonene, and perillyl alcohol to create meth(acrylate)-free systems for DLP printing *via* thiol–ene reactions.[70,75,76] While the presence of ester bonds in these materials facilitates degradation *via* hydrolysis, they break down to form innocuous byproducts that cannot be recured or recycled into resins without prior modification. To overcome end-of-life issues, incorporation of dynamic covalent bonds represents a promising approach to design renewable and recyclable networks for a circular plastic economy.[77–79] Bioderived lipoic acid, containing a dynamic strained cyclic disulfide, has been leveraged in resins for DLP printing for the development of reprocessable networks and thermoplastics.[27,63] However, the inclusion of diacrylates and other vinyl monomers in resins to facilitate printing renders these materials non-depolymerizable, with recycling relying on the addition of reactive species at each recurring step. To address this limitation, Dove and coworkers developed a resin that combines monofunctional and multi-arm lipoate monomers that upon light irradiation form soft dynamic networks that can be depolymerized and directly re-cured *via* DLP printing (Fig. 2E).[80]

Growing environmental awareness has also motivated AM companies such as FormLabs, Photocentric, and Carbon to develop a new generation of bio-based resins that require a lower carbon footprint for manufacturing.[81–83] Although resin formulations are usually not revealed, Photocentric has disclosed the use of the monoterpene camphene as a precursor to form renewable functional reactive diluents and oligomers.[82] Ultimately, the sustainable AM market is still in its infancy with challenges associated with scalability, economic viability, and lack of end-of-life analysis. Optimizing the delicate balance between performance and processability is crucial for realizing the full potential of bio-based, sustainable resins. Furthermore, photoinitiators can be toxic to biological systems and environment and therefore increasing efforts have been focused on developing photoinitiator-free chemistries (*e.g.*, maleimides,[84] photocaged thiols,[85] coumarins,[86] diazirines,[87] anthracenes[88]) to chart a new way forward.[89]

Employing bio-based resins to engineer living systems

In contrast to bio-derived resins, which contain components derived from natural feedstock with a focus towards sustainability, 'bio-based' resins or bioinks, as defined here, are designed to host living matter such as cells to create engineered living systems. Examples of engineered living systems enabled by VP include healthcare materials such as patient-specific organ-conforming hydrogel patches,[90] 3D scaffolds for regenerative medicine[91] and *in vitro* models for disease modeling and drug screening.[92] In addition to mammalian cells, engineered host materials with open architectures can be designed to support growth of genetically modified microorganisms such as bacteria, mycelium, or yeast (Fig. 2F)[93–95] for specific functions such as photosynthesis for carbon sequestration.[96] 3D printing is an advantageous platform technology in these applications because of the ability to customize open-lattice scaffolds or perfusable channels for fluid transport. This flexibility can aid with the incorporation of multiple cells or matrix components in a predefined spatial manner or engineering porosity to guide cell infiltration, recently outlined in a review by Burdick and coworkers.[3]

Successful fabrication of engineered living systems using VP relies on the design of cytocompatible, aqueous bioresins, which typically contain lower polymer concentrations than conventional photoresins to provide a suitable environment for living cells. Acrylate-functionalized gelatin and poly(ethylene glycol) are commonly employed macromers for bioresins,[97] but chemical modifications of other biopolymers (*e.g.*, hyaluronic acid, silk, alginate, cellulose, chitosan) can also be used to form hydrogels, owing to their innate biodegradability, bioactivity, low immunogenicity, and biocompatibility.[3,19]

The high water content within hydrogels that enables functionality can also lead to several challenges with implementation. Disadvantages such as batch-to-batch variability and dispersity in molecular weights can affect both functionalization degree and crosslinking kinetics of biopolymers. Resins with high water content also tend to have high D_p, which can lead to overcuring, and rapid diffusion of intermediates, which can lead to cross-linking reactions beyond desired voxels. Finally, a major challenge in the translation of 3D printed biopolymer hydrogels for load-bearing applications has been the poor mechanical strength of such hydrogels; while high water content materials are generally soft, 3D printed hydrogels also tend to be brittle.

To improve the utility of biopolymers and hydrogels used in engineered living systems, development of tougher host materials should be explored, for example *via* mechanical reinforcement by incorporating additional physical crosslinks or secondary networks.[98] To improve print resolution, continued development of cytocompatible radical scavengers or aqueous photoabsorbers is warranted, and computational strategies to mitigate cell-induced light scattering could

further improve the resolution of printed complex structures.[99] Additionally, predicting material changes, such as cell-driven degradation or reinforcement from secreted biomolecules, will be vital for maintaining functionality over time. Success in these areas will enable the creation of more complex, hierarchical structures that meet the demands of both medical and environmental applications.

4. Developing new processes for VP

In addition to innovations in chemistry, design and implementation of new processing methods are needed to push the boundaries of VP. These methods can integrate complex hardware with novel optical configurations to address challenges in VP and enhance functionality of the printed materials. Here, we outline key limitations and recent advances at the forefront of developing new processes.

Overcoming the mechanical performance-processability conflict

A persistent challenge associated with VP is the gradient in monomer conversion due to short exposure times, use of photoabsorbers, oxygen inhibition, and diffusion limitations can reduce the overall mechanical properties of 3D printed materials when compared to those fabricated by traditional casting or molding. Therefore, efforts are being made to resolve this processability-performance tradeoff in 3D printing. Typical DLP resins must be low viscosity to prevent part delamination due to Stefan adhesion forces, promote rapid refill of the void space formed by the separation of each printed layer from the resin vat, and enable high resolution printing. The workable viscosity range for a DLP resin is often described as <10 Pa s or 10 000 cP, which is significantly lower than typical viscosities of polymer solutions.[29,100] Modification of printing setup (*e.g.*, equipping resin vats with heaters to reduce viscosity) has been demonstrated but requires specialized equipment and may be challenging to implement with temperature-sensitive materials. Another approach to reducing viscosity is to add reactive diluents or solvents. Unfortunately, incorporation of reactive diluents into resins can significantly limit control over mechanical properties and degradability of printed objects, whereas solvents can cause printed objects to experience anisotropic shrinkage, cracking, or warping as the solvent evaporates. To address these limitations, Becker and coworkers demonstrated an alternative approach involving the use of low-viscosity degradable polymers for solvent free 3D printing under ambient conditions.[29] Taking inspiration from bottlebrush polymer architectures, this approach leverages synthetic polymers with short side chains that prevent chain entanglement and thus promote low viscosity ambient behavior. Printed objects from these solvent free resins display tunable mechanical properties based on chain length and extent of crosslinking and exhibit minimal shrinkage. While ambient, solvent free DLP printing is promising, this technique still requires relatively low molecular weight polymers to ensure low viscosities and therefore leads to 3D printed materials with compliant mechanical properties.

One mechanism for enhancing mechanical strength is through polymer chain entanglements that act as slip crosslinks.[101] However, obtaining dense entanglements requires crowding of high molecular weight polymer chains at high concentrations. 3D printing of precursors with preexisting entanglements through vat photopolymerization is challenging due to their high viscosity making them incompatible particularly with DLP. To overcome this limitation, one strategy has been to 3D print with low viscosity resin containing a high concentration of monomers and extremely low concentrations of crosslinker and photoinitiator to densely entangle the polymer chains as they form. This can be readily executed through a new method called continuous curing after light exposure aided by redox initiation (CLEAR) developed by Burdick and coworkers.[102] With this approach, DLP sets the shape of the printed object whereas a complementary redox reaction (dark polymerization) allows complete conversion of any unreacted monomer in a slow, steady manner within the printed object (Fig. 3A). CLEAR can be implemented to form highly entangled hydrogels and elastomers and can be adopted with both aqueous and organic or solvent-free systems by simply adding the redox initiators within the resin right before 3D printing.[102] In addition to providing enhanced mechanical properties, CLEAR printing opens avenues for 3D customizability when considering applications of hydrogels as tissue adhesives. As an example, this technique can be used to spatially pattern tissue adhesive and non-adhesive regions within a hydrogel to enable use in applications like removable medical devices.[102]

Another approach to processing high molecular weight polymer solutions has been with the use of colloidal particles with diameter ranging between 100 and 1000 nm. Colloidal polymeric particles decouple the molecular weight-viscosity relationship by sequestering polymer chains into a discrete phase, thereby limiting intermolecular interactions such as entanglements.[103] In this context, Long, Williams and coworkers illustrated a novel platform leveraging colloids to DLP print high molecular weight latex resins that were once deemed unprintable.[103] Photocrosslinking of water-soluble network precursors in the continuous phase forms a robust template that surrounds the latex particles. Subsequent post-processing (*e.g.*, dehydration under mild conditions) promotes 3D coalescence of the latex particles throughout the printed scaffold, resulting in a semi-interpenetrating polymer network and imparting elastomeric properties. This approach has been expanded to include waterborne polyurethanes, synthetic isoprene rubber, natural rubber, ABA triblock copolymer poly(styrene-*b*-isoprene-*b*-styrene), and olefinic elastomer ethylene–propylene–diene monomer rubber, demonstrating the extensive range of material properties attainable by varying the colloidal polymer.[104–107] By employing strategic chemical design, future directions for these platforms can include the incorporation of ionic moieties to effectively stabilize polymer particles in an aqueous media and reduced viscosities for facile processing.

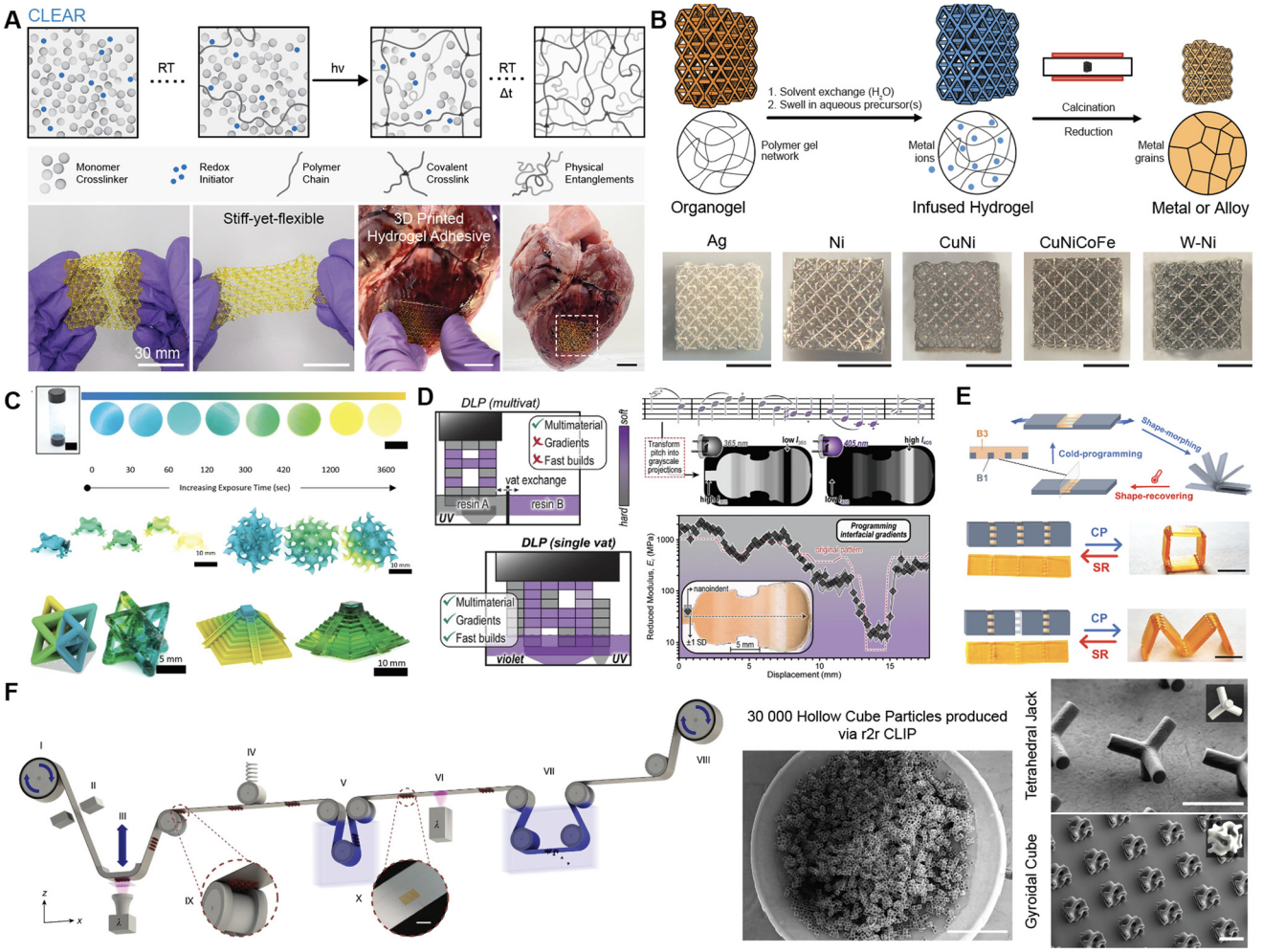

Fig. 3 Development of new processing methods for VP of functional materials. (A) Schematic representation of continuous curing after light exposure aided by redox initiation (CLEAR) printing of highly entangled polymer networks. Photographs of CLEAR printed stiff-yet-conformable porous patch that are extensible and can be adhered to porcine heart in the presence of blood. (B) Schematic representation of hydrogel infusion additive manufacturing (HIAM) process and optical images of metals (Ag and Ni), binary alloy (CuNi), high entropy alloy (CuNiCoFe) and refractory alloy (W-Ni) lattices. (C) Exploration of color flexibility of resin upon exposure to 365 nm light for varied exposure times and subsequent alterations in color of 3D printed structures (frog and gyroid) upon exposure to 365 nm light. Dual-wavelength VP for 3D printing of gradient multi-color objects (octet truss and pyramid). (D) Schematic comparison of multi-material printing using multi- or single vat approach. Complex grayscale gradient of stiffness corresponding to a violin excerpt. Nanoindentation of the 3D printed gradient overlaps with the theoretical stiffness value. (E) Schematic representation of the heterogeneous hinge module design and morphing. Cold-programming (CP) and shape recovery (SR) of grayscale DLP printed structures. (F) Schematic representation of the experimental setup for roll-to-roll (r2r) CLIP wherein particles are fabricated onto an aluminum coated PET film and undergo washing, secondary curing, and harvesting in a quasi-continuous manner. Scanning electron microscope images to demonstrate scalability (30 000 hollow cube particles) and other complicated geometries like tetrahedral jacks and gyroidal cubes fabricated *via* r2rCLIP. Adapted with permission from (A),[102] (B),[113] (C),[129] (D),[144] (E),[156] (F).[173]

Leveraging reactive conversion for functional materials

Thermal conversion of 3D printed soft materials (*e.g.*, polymers with reactive fillers) can drive material transformations that enable fabrication of high-value components including ceramics,[108,109] glassy carbon,[110] silica glasses,[111,112] and metals[113] that are useful in diverse applications ranging from the biomedical to aerospace fields. Taking advantage of reactive conversion methods to fabricate non-polymeric materials is desirable when methods for directly 3D printing such materials do not exist. There is a growing body of work in which photopolymers themselves are used as precursors in pyrolysis processes that yield architected carbon materials.[114–116] However, reactive conversion techniques often rely on incorporation of target fillers or dispersion of particles into the photoresin, resulting in a heterogeneous slurry. Such resins tend to be viscous, requiring active recoating. Furthermore, suspended particles scatter or absorb light, leading to difficulties with curing. To avoid design challenges associated with incorporation of target precursors in the photoresin,[117] Greer and co-workers introduced hydrogel infusion additive manufacturing (HIAM).[113] HIAM is a simple and

accessible approach that enables fabrication of a wide variety of metals (*e.g.*, copper, nickel, tungsten, and multicomponent alloys) from a single photoresin by infusing precursors into gels after printing (Fig. 3B).[113] For instance, 3D printing of copper metal is particularly challenging at the sub-millimeter scale using conventional laser-based sintering techniques due to its high thermal conductivity; HIAM enables fabrication of copper metal with feature sizes below 50 μm. In the future, HIAM can open avenues for applications such as electrodes for water splitting or battery current collectors. Since diffusion of reactive precursors in a printed gel is critical for HIAM, subsequent work can focus on engineering specific binding interactions into the gel to enable high mass loading of precursors during infusion.[118,119] Holistic understanding of mass transport and chemical transformation processes *via* real-time characterization of conversion processes will be of fundamental importance towards structure–property optimization. Finally, with scale-up of reactive conversion AM, special emphasis should be placed on sustainability regarding the choice of sacrificial polymer and methods to recover and utilize pyrolysis byproducts.

Introducing and controlling nanoarchitecture

Additional shape complexity for vat polymerization can be achieved by polymerization induced phase separation (PIPS) which adds nano- to micro-meter porosity, gradients, or functionalization to printed structures.[120] PIPS can be leveraged with VP by creating resins that contain homogenously mixed porogens (*e.g.*, solvents) and monomers; but upon photopolymerization, the system phase separates into polymer-rich and polymer-poor phases.[121,122] Post-printing, these porogens can be exchanged and the structures can be dried with critical point drying to leave empty voids. This hierarchical control allows for changes to bulk mechanical properties, diffusive properties, surface area, and density of materials. For instance, Page and coworkers combined DLP with PIPS to fabricate materials with tunable pore sizes (in the range of 100 to 270 nm) and demonstrate tunability of flow properties (*i.e.* flux and diffusion) as structured sorbents for recycling.[123] Looking forward, this technique can be applied for drug delivery and tissue engineering to create porous networks with controlled release profiles by tuning pore size and structure geometry. By adjusting porogen feed parameters in a resin during printing, gradients in porosity may be achieved. Multi-vat and grayscale vat polymerization also offer exciting avenues for fabricating multi-scale porous materials with spatially varied properties. Additionally, developing tougher material systems could broaden the use of PIPS for creating functional foam materials.

Enhancing complexity *via* intensity or wavelength modulation

Drawing inspiration from nature's ability to create composite materials with disparate and finely tuned mechanical properties, synthetic multi-material 3D structures hold transformative potential in biomimetics, soft robotics, and biomedical applications. Yet, challenges in material chemistry and manufacturing techniques continue to limit the precise, rapid production of such complex multi-material designs. Traditional multi-material VP techniques typically rely on multiple resin vats to introduce material heterogeneity.[124] Multi-material printing *via* resin exchange can be challenging due to constraints associated with hardware modifications and complex washing protocols that reduce print speeds and lead to waste and cross-contamination. Recently, Soman and coworkers reported a new vat-free printing platform that relies on generating and maintaining a resin meniscus between a crosslinked structure and bottom window to print lateral, vertical, discrete, or gradient multi-material 3D structures.[125] Another approach to multi-material printing is the use of grayscale light projection.[126,127] Grayscale DLP methods use a single light source with light intensity modulation to create continuous mechanical gradients, producing structures with gradual modulus changes that enable finely tuned multi-modulus architectures using simple chemistries. However, it is challenging to design a chemical system based in a single vat that results in multiple materials. An alternative to modulating intensity of a single wavelength light is printing with multiple wavelengths of light; so-called dual-wavelength or multi-color printing presents opportunities to enhance complexity in material properties, functionality, and chemical composition throughout the cured volume.[128,129] This technique requires the use of a photoresin that responds differently to each irradiated wavelength. The irradiation modes that can be employed during dual color irradiation include synergistic (λ_1 and λ_2 lead to curing), cooperative (λ_1 and/or λ_2 lead to curing), orthogonal (λ_1 or λ_2 lead to curing), and antagonistic (λ_1 and not λ_2 lead to curing).[130,131] Current advances in the field of multi-color printing rely mainly on cooperative curing, whereby one wavelength causes one process to trigger (*e.g.* radical curing) and another wavelength causes both that process and a secondary one (*e.g.* radical along with cationic).[132,133] For instance, Boydston and coworkers achieved multi-material VP using acrylate- and epoxide-based monomers that can undergo simultaneous radical and cationic polymerizations using visible and UV light, respectively.[128] Further, multi-wavelength printing using visible and UV wavelengths can be used to cure and impart color to each layer, respectively. Incorporation of photoacid generator allows control over local acidity and therefore, optical color of a pH-responsive dye upon irradiation of resin with UV light (Fig. 3C).[129] When printing with multiple colors, it is important to understand and identify wavelength regimes that enable full wavelength orthogonality in the reactivity. Barner-Kowollik and coworkers have established the photochemical action plot methodology, a technique that maps the photochemical reactivity of a system wavelength-by-wavelength. Remarkably, the wavelength-dependent reactivity of a photosystem often reaches a maximum at a wavelength that is mismatched (often red-shifted) when compared to the absorption spectrum of the reacting chromophore.[131,134,135] Several wavelength-orthogonal reaction manifolds have been discovered for bond-forming reactions (*e.g.*, cooperative network formation[136,137] or photodimeriza-

tions[138]). Incorporating orthogonal chromophores into the backbone of pre-polymers can enable multi-wavelength VP without the need for radical or cationic initiators.[139,140] This technique has been recently used to develop a single photoresin that allows the printing of two completely different materials depending only on the wavelength used and is enabled with the use of a custom-made stereolithographic printer coupled to a monochromatic tuneable laser (MonoLISA).[141] This methodology expands the possibilities of multi-wavelength printing from materials with regions of different mechanical properties to tuneable smart materials with programmable degradability.[141] Wavelength-orthogonal reaction manifolds can also add complexity other than merely printing multi-material structures. For example, wavelength-orthogonal cargo release systems present opportunities to print functional materials for biomedical applications,[142] and photodimerizations have been used to show wavelength-orthogonal modulation of material properties in hydrogels.[143] Identification and scalable synthesis of orthogonal chromophores remain primary challenges in developing wavelength-orthogonal resins. Page and coworkers combined multi-color and grayscale to spatially control composition and material properties within a single structure.[144] This technique integrates color-selective initiators that can trigger distinct polymerization mechanisms: UV (365 nm) exposure initiates a rigid, crosslinked network *via* radical chain growth, while visible (405 nm) light produces a softer, lightly crosslinked network through an anionic step-growth mechanism (Fig. 3D). Grayscale control further enhances the process by allowing programmable stiffness gradients (up to 150-fold changes in stiffness across interfaces) effectively mimicking modulus transitions as seen in human tendons.[144] Future investigations can also include expanding multi-material printing to inorganic materials. Looking ahead, multi-material approaches open opportunities to incorporate additional photo-polymerization mechanisms, including radical, anionic, and cationic chemistries, broadening the range of mechanical properties and facilitating practical applications for medical devices and flexible electronics.

Engineering dynamic responsiveness

4D printing refers to AM of stimuli-responsive materials where the application of a stimulus (*e.g.*, heat, light, humidity, pH) can (i) effect a change in shape or mechanical properties of a 3D-printed object or (ii) confer the capability to switch between two or more multiple programmed states or (iii) allow self-healing.[145,146] In another instance, using dynamic covalent chemistries like alkoxyamine bonds can enable growth (chain extension by nitroxide-mediated polymerization) and degrowth (reversible homolysis *via* nitroxide exchange reactions) of printed structures to control size and modulus at a later time.[147] 4D printing materials with degradable groups can be actuated by chemical stimuli, such as varying pH,[148–150] temperature,[84] or enzymatic degradation.[151] Using light as the degradation stimulus provides spatiotemporal control over material softening or degradation, which can enable fabrication of precise negative features such as high-resolution microfluidic channels that are often challenging to print *via* DLP due to overcuring between layers. Therefore, creating resins that include orthogonal polymerization and depolymerization functionalities can be helpful to create negative features within a printed object by *via* photo-degradation.[152] For instance, *o*-nitro-benzyl (*o*NB) functionality can be incorporated within printed high-resolution microstructures and be subsequently leveraged to create negative features by cleaving the *o*NB moieties with 365 nm light.[152] Such an approach can be used to fabricate complex constructs like vascular networks with multi-scale resolution from centimeter (AM) to single-digit micrometer (two-photon ablation) features.[153] For instance, sequential additive (CLIP) and subtractive (multiphoton ablation) steps can create hollow features within a 3D object at any depth overcoming issues with light penetration depth.[154] This method could also be applied to an adaptive manufacturing VP system, where regions of overcure could be removed to more precisely match the projection. In addition to light, its absence (*i.e.* darkness) can also be used to trigger the degradation of printed structures with spatially programmed degradability and light-stabilization.[139] Nevertheless, there are very few reports of VP resins that feature both polymerization and depolymerization mechanisms spatially controlled by light. This is largely due to the inherent photocrosslinking-photodegradation tradeoff wherein using light to form an object can cause premature degradation of the photoresponsive groups. Therefore, new strategies for VP of photoresponsive materials using wavelength-orthogonal reactions are needed. Such advancements could enable hybrid additive and subtractive manufacturing of precise multi-scale structures for microfluidics, batteries, and general applications to closed-loop adaptive manufacturing systems.

Beyond degradation-mediated responsiveness, shape transformations can be realized with 3D printed shape memory polymers (SMP) or liquid crystal elastomers (LCEs) that are capable of rapid, reversible shape change upon application of stimuli.[146,155] To achieve the shape memory cycle, SMPs need to undergo a programming and subsequently a recovery step. Qi and coworkers leveraged grayscale DLP to print materials ranging from ductile glassy thermosets to highly stretchable organogels with tunable elasticities and glass transition temperatures using a single vat of resin.[156] This single-vat multi-property printing platform enables fabrication of cold-programmable SMPs structures with varying distribution and direction of the modular hinges that can undergo shape morphing into multiple configurations at room temperature (Fig. 3E). In contrast, AM of LCEs has mainly focused on its use with the direct ink writing (DIW) technique due to its inherent capability to align LCEs through shear developed during the extrusion process. However, growing body of research has explored fabrication of LCEs using DLP. Alignment of LCEs can be achieved by using a variable direction magnetic field (*e.g.*, integrated Halbach array) into a DLP resin vat.[157] Controlling alignment directions for different layers allows for programming of layers within the 3D printed

object, thereby enabling more complex modes of actuation. In addition to magnetic field alignment, DLP printing of LCEs has incorporated shear alignment to achieve unidirectionally-aligned parts using hybrid approaches that combine DIW with VP.[158,159] Further, DLP of LCEs has expanded the envelope of printable materials to create objects that actuate upon exposure to heat or different wavelengths of light.[160] In addition to DLP, Blasco and coworkers have recently demonstrated the use of two-photon laser printing for alignment of LCEs under confinement[161] and microscale fabrication of 4D photoresponsive LCE actuators.[162] As an example, traditional methods for fabrication of LCE actuators use azobenzene dyes with a photopolymerizable group in the LC ink during printing, however, incorporating dyes into microstructures post-3D printing avoids incompatibilities with the presence of dyes during printing and allows single- and multi-color actuation at wavelengths ranging from 400 to 650 nm.[162] While VP has immense potential for fabrication of stimuli-responsive materials, its success requires further development in both hardware for improved alignment of LCEs and materials chemistry to enhance functionality. Further, developing new approaches for spatial alignment of LCEs using cheap, commercially available setups at lower field strength can lower the entry barrier for complex 3D prints.

For applications that may require *in vivo* actuation or bioprinting, delivery of UV or visible light may pose intrinsic challenges due to low penetration depths within optically scattering media such as biological tissues. Therefore, future research of VP systems that utilize infrared (IR) light source (at wavelengths longer than 850 nm) is needed.[86,163] Beyond using light as part of vat photopolymerization, there has been a growing interest in the use of other modalities such as ultrasound to trigger polymerization reactions[164] or generate intricate patterns within composite materials.[165] Looking ahead, integrating such advanced patterning techniques (*e.g.*, acoustic, ultrasonic, magnetic, or electric fields) with VP can open avenues for applications in biomedical, healthcare, energy, and sustainability fields.[166]

Navigating the scalability barrier

The progress in VP including innovative resin designs and novel instrumentation approaches has been essential in providing customizability and freeform fabrication capabilities. To be adopted in commercial fabrication, VP methods must compete with the rapid throughput of conventional manufacturing techniques like injection molding. A framework for contextualizing resolution and throughput relationships in the VP field was recently proposed by Shusteff and coworkers, highlighting a critical balance between build rate, feature size, and build volume necessary for achieving scalability.[167] Applications such as biomicrofluidics or architected energy materials often require centimeter-scale devices with microscale feature resolution which are difficult to obtain with VP due to the print resolution-build size tradeoff. To overcome this conflict, strategies based on the use of spatial light modulator combined with an optical scanning system or light-sheet 3D printing can be employed to produce microscale features over a large area at rapid rates.[168,169] In an alternate approach, multi-path projection SLA designed to switch between high resolution (~10 μm) and low resolution (~30 μm) optical paths was leveraged to generate centimeter sized constructs (3 × 6 cm) with 10 μm feature resolution.[170] Achieving industrial scalability requires a comprehensive evaluation of VP contextual performance and post-print processing requirements. Post-print processing is often an overlooked yet essential factor in scalability; a technique that reduces fabrication time at the cost of increasing post-processing time may not improve overall production efficiency. Therefore, developing integrated, orthogonal, or decoupled fabrication platforms is imperative. Such methods can reduce manual processing steps, minimize material waste, enable parallel part processing, and increase the repeatability of material properties and component performance. One approach for scalable production has been continuous printing within a flow channel.[171] Recent efforts have focused on pushing the resolution limit down to single digit micrometer scale while maintaining high-throughput (10^6 unit-sized components per day) requirements essential for precision manufacturing.[172] As an example, roll-to-roll CLIP (r2rCLIP), introduced by DeSimone and coworkers, provides a platform approach to quasi-continuously produce components in a conveyor belt process (Fig. 3F).[173] This technique substitutes a roll of aluminum-coated polyethylene terephthalate for a traditional, static build platform. An array of hundreds of components is fabricated simultaneously on the film, which is then translated laterally. Subsequent arrays can be fabricated while previous arrays undergo in-line post-processing steps such as washing, secondary curing, and harvesting. This technique enables applications ranging from soft hydrogels for pulsatile drug delivery to hard ceramics for advanced microtool geometries. Moreover, rapid AM on a roll-based process is laterally expandable with other in-line rapid techniques (such as iCLIP).[174] Future orthogonal, industrially relevant modifications can include parallelized printing multiplication (copies of arrays simultaneously on a wider belt), in-line quality characterization and part verification, and machine-learning based real-time parameter feedback. Initial industrial steps towards this modality have recently arisen *via* introduction of print-harvest-print upgrades including Carbon's M3 Max Automatic Operation Backpack and Formlabs' Form Auto. Commercialization and large-scale VP can benefit from efforts to automate print preparation (with user-friendly design engines and machine learning algorithms to optimize layout of multiple parts within the build volume) and real-time prediction, monitoring, and optimization of the printing process. For instance, separation forces in VP can be predicted,[175] measured *via* online force monitoring,[176] and optimized *via* deep learning.[177] Another powerful tool to monitor print interfaces in real time with micron-scale resolution is optical coherence tomography (OCT), which can be used to monitor process parameters such as interface deflections, flow fields, and polymerization fronts.[2]

5. Conclusion

Vat photopolymerization additive manufacturing (AM) is a field in a moment of coalescence, emphasized by the recent addition of polymer-focused AM conferences such as the GRC on Additive Manufacturing of Soft Materials. This perspective combines ideas from researchers from diverse backgrounds (chemistry, physics, engineering, and material science) to highlight the recent progress in the field of VP. The varied discussions presented in this work help to broadly sketch out a holistic framework for the advancing directions and highlight the voices of researchers at an early stage of their career. Areas of critical importance identified by the group include standardizing best practices for resin design to ensure reproducibility and transparency, as well as developing novel chemistries compatible with VP, going beyond conventional acrylate-based resins to radical-free systems, employing bio-based systems, and resins that are circular and sustainable. Finally, novel processing approaches, including printer design for scalability and post-processing approaches that enable a wider variety of "previously impossible" materials to be 3D printed using VP are discussed. By innovating across technical boundaries and building bridges across disciplines, we hope to set the stage for continued creativity, growth, and success of the VP community.

Author contributions

A.P.D. and M.A.S. conceived of the concept and edited the manuscript. Each author contributed expertise to write the following sections: A.P.D., post-processing strategies; R.H.B., latex printing; V.C., circular and sustainable resins; A.J.C., thermoplastic printing; D.D., bio-based resins and engineered living systems; H.E.F., ring-opening metathesis polymerization; J.M. F., multi-wavelength, multi-material printing; H.H., 4D printing; T.K., Diels–Alder photopatterning; J.-W.K., multi-wavelength, multi-material printing; J.M.K., scalability and best practices for resin design; K.S.M., polymerization induced phase separation; C.J.O., triplet–triplet annihilation upconversion; F.P.-J., multi-wavelength, multi-material printing; D.H.P., 4D printing; M.I.S., solvent-free printing and click reactions; S. Y., bio-derived sustainable feedstocks; M.A.S., reactive conversion. All authors provided feedback and approved the manuscript for submission.

Data availability

No primary research results, software, or code have been included, and no new data were generated or analyzed as part of this perspective.

Conflicts of interest

The authors declare no conflicts of interest.

Acknowledgements

All authors acknowledge the support of their supervisors, who approved the early-career researcher focus of this manuscript. H. E. F. acknowledges support from the Laboratory Directed Research and Development program at Sandia National Laboratories, a multimission laboratory managed and operated by the National Technology and Engineering Solutions of Sandia, LLC, a wholly owned subsidiary of Honeywell International, Inc., for the U.S. Department of Energy's National Nuclear Security Administration under contract DE-NA-0003525. F. P.-J. acknowledges Queensland University of Technology (QUT) and UGent for PhD scholarship. J. M. K. acknowledges support from National Science Foundation Graduate Research Fellowship Program (DGE-1656518) and Bill & Melinda Gates Foundation (No. INV-046940). Partial support was provided by the Robert A. Welch Foundation (F-2007) to J.-W. K., K. S. M., C. J. O., H. H. and D. H. P. acknowledge this work was performed under the auspices of the U.S. Department of Energy by Lawrence Livermore National Laboratory under Contract DE-AC52-07NA27344, LLNL-JRNL-872583. Parts of Figure 1 were designed in BioRender.

References

1 P. Somers, A. Münchinger, S. Maruo, C. Moser, X. Xu and M. Wegener, *Nat. Rev. Phys.*, 2023, **6**, 99–113.
2 G. Lipkowitz, M. A. Saccone, M. A. Panzer, I. A. Coates, K. Hsiao, D. Ilyn, J. M. Kronenfeld, J. R. Tumbleston, E. S. G. Shaqfeh and J. M. DeSimone, *Proc. Natl. Acad. Sci. U. S. A.*, 2024, **121**, e2303648121.
3 A. P. Dhand, M. D. Davidson and J. A. Burdick, *Nat. Rev. Bioeng.*, 2025, **3**, 108–125.
4 C. Greant, B. Van Durme, J. Van Hoorick and S. Van Vlierberghe, *Adv. Funct. Mater.*, 2023, **33**, 2212641.
5 S. C. Gauci, A. Vranic, E. Blasco, S. Bräse, M. Wegener and C. Barner-Kowollik, *Adv. Mater.*, 2024, **36**, 2306468.
6 V. Hahn, N. M. Bojanowski, P. Rietz, F. Feist, M. Kozlowska, W. Wenzel, E. Blasco, S. Bräse, C. Barner-Kowollik and M. Wegener, *ACS Photonics*, 2023, **10**, 24–33.
7 P. Müller, R. Müller, L. Hammer, C. Barner-Kowollik, M. Wegener and E. Blasco, *Chem. Mater.*, 2019, **31**, 1966–1972.
8 B. Grigoryan, S. J. Paulsen, D. C. Corbett, D. W. Sazer, C. L. Fortin, A. J. Zaita, P. T. Greenfield, N. J. Calafat, J. P. Gounley, A. H. Ta, F. Johansson, A. Randles, J. E. Rosenkrantz, J. D. Louis-Rosenberg, P. A. Galie, K. R. Stevens and J. S. Miller, *Science*, 2019, **364**, 458–464.
9 J. R. Tumbleston, D. Shirvanyants, N. Ermoshkin, R. Janusziewicz, A. R. Johnson, D. Kelly, K. Chen, R. Pinschmidt, J. P. Rolland, A. Ermoshkin, E. T. Samulski and J. M. DeSimone, *Science*, 2015, **347**, 1349–1352.
10 D. A. Walker, J. L. Hedrick and C. A. Mirkin, *Science*, 2019, **366**, 360–364.

11 M. Shusteff, A. E. M. Browar, B. E. Kelly, J. Henriksson, T. H. Weisgraber, R. M. Panas, N. X. Fang and C. M. Spadaccini, *Sci. Adv.*, 2017, **3**, 5496.
12 B. E. Kelly, I. Bhattacharya, H. Heidari, M. Shusteff, C. M. Spadaccini and H. K. Taylor, *Science*, 2019, **363**, 1075–1079.
13 G. Größbacher, M. Bartolf-Kopp, C. Gergely, P. N. Bernal, S. Florczak, M. de Ruijter, N. G. Rodriguez, J. Groll, J. Malda, T. Jungst and R. Levato, *Adv. Mater.*, 2023, **35**, 2300756.
14 D. Ribezzi, M. Gueye, S. Florczak, F. Dusi, D. de Vos, F. Manente, A. Hierholzer, M. Fussenegger, M. Caiazzo, T. Blunk, J. Malda and R. Levato, *Adv. Mater.*, 2023, **35**, 2301673.
15 M. B. Riffe, M. D. Davidson, G. Seymour, A. P. Dhand, M. E. Cooke, H. M. Zlotnick, R. R. McLeod and J. A. Burdick, *Adv. Mater.*, 2024, 2309026.
16 M. Regehly, Y. Garmshausen, M. Reuter, N. F. König, E. Israel, D. P. Kelly, C. Y. Chou, K. Koch, B. Asfari and S. Hecht, *Nature*, 2020, **588**, 620–624.
17 C. Vidler, M. Halwes, K. Kolesnik, P. Segeritz, M. Mail, A. J. Barlow, E. M. Koehl, A. Ramakrishnan, L. M. Caballero Aguilar, D. R. Nisbet, D. J. Scott, D. E. Heath, K. B. Crozier and D. J. Collins, *Nature*, 2024, **634**, 1096–1102.
18 S. C. Ligon, R. Liska, J. Stampfl, M. Gurr and R. Mülhaupt, *Chem. Rev.*, 2017, **117**, 10212–10290.
19 K. S. Lim, J. H. Galarraga, X. Cui, G. C. J. Lindberg, J. A. Burdick and T. B. F. Woodfield, *Chem. Rev.*, 2020, **120**, 10662–10694.
20 T. J. Kolibaba, J. P. Killgore, B. W. Caplins, C. I. Higgins, U. Arp, C. C. Miller, D. L. Poster, Y. Zong, S. Broce, T. Wang, V. Talačka, J. Andersson, A. Davenport, M. A. Panzer, J. R. Tumbleston, J. M. Gonzalez, J. Huffstetler, B. R. Lund, K. Billerbeck, A. M. Clay, M. R. Fratarcangeli, H. J. Qi, D. H. Porcincula, L. B. Bezek, K. Kikuta, M. N. Pearlson, D. A. Walker, C. J. Long, E. Hasa, A. Aguirre-Soto, A. Celis-Guzman, D. E. Backman, R. L. Sridhar, K. A. Cavicchi, R. J. Viereckl, E. Tong, C. J. Hansen, D. M. Shah, C. Kinane, A. Pena-Francesch, C. Antonini, R. Chaudhary, G. Muraca, Y. Bensouda, Y. Zhang and X. Zhao, *Addit. Manuf.*, 2024, **84**, 104082.
21 B. W. Caplins, T. J. Kolibaba, U. Arp, C. C. Miller, Y. Zong, D. L. Poster, C. I. Higgins and J. P. Killgore, *Addit. Manuf.*, 2024, **85**, 104172.
22 J. Bennett, *Addit. Manuf.*, 2017, **18**, 203–212.
23 R. Levato, O. Dudaryeva, C. E. Garciamendez-Mijares, B. E. Kirkpatrick, R. Rizzo, J. Schimelman, K. S. Anseth, S. Chen, M. Zenobi-Wong and Y. S. Zhang, *Nat. Rev. Methods Primers*, 2023, **3**, 1–19.
24 J. J. Schwartz, *MRS Bull.*, 2022, **47**, 628–641.
25 M. T. Kiker, A. Uddin, L. M. Stevens, C. J. O'Dea, K. S. Mason and Z. A. Page, *J. Am. Chem. Soc.*, 2024, **146**, 19704–19709.
26 X. Lopez de Pariza, O. Varela, S. O. Catt, T. E. Long, E. Blasco and H. Sardon, *Nat. Commun.*, 2023, **14**, 1–11.
27 C. Choi, Y. Okayama, P. T. Morris, L. L. Robinson, M. Gerst, J. C. Speros, C. J. Hawker, J. Read de Alaniz and C. M. Bates, *Adv. Funct. Mater.*, 2022, **32**, 2200883.
28 Y. Shin and M. L. Becker, *Biomacromolecules*, 2022, **23**, 2106–2115.
29 M. I. Segal, A. J. Bahnick, N. G. Judge and M. L. Becker, *Angew. Chem., Int. Ed.*, 2024, e202414016.
30 M. Zhong, R. Wang, K. Kawamoto, B. D. Olsen and J. A. Johnson, *Science*, 2016, **353**, 1264–1268.
31 A. V. Dobrynin, Y. Tian, M. Jacobs, E. A. Nikitina, D. A. Ivanov, M. Maw, F. Vashahi and S. S. Sheiko, *Nat. Mater.*, 2023, **22**, 1394–1400.
32 B. E. Kirkpatrick, G. K. Hach, B. R. Nelson, N. P. Skillin, J. S. Lee, L. P. Hibbard, A. P. Dhand, H. S. Grotheer, C. E. Miksch, V. Salazar, T. S. Hebner, S. P. Keyser, J. T. Kamps, J. Sinha, L. J. Macdougall, B. D. Fairbanks, J. A. Burdick, T. J. White, C. N. Bowman and K. S. Anseth, *Adv. Mater.*, 2024, **36**, 2409603.
33 K. M. Dawood and K. Nomura, *Adv. Synth. Catal.*, 2021, **363**, 1970–1997.
34 A. J. Greenlee, R. A. Weitekamp, J. C. Foster and S. C. Leguizamon, *ACS Catal.*, 2024, **14**, 6217–6227.
35 J. C. Foster, A. W. Cook, N. T. Monk, B. H. Jones, L. N. Appelhans, E. M. Redline and S. C. Leguizamon, *Adv. Sci.*, 2022, **9**, 2200770.
36 S. Kovačič and C. Slugovc, *Mater. Chem. Front.*, 2020, **4**, 2235–2255.
37 S. C. Leguizamon, K. Lyons, N. T. Monk, M. T. Hochrein, B. H. Jones and J. C. Foster, *ACS Appl. Mater. Interfaces*, 2022, **14**, 51301–51306.
38 A. K. Rylski, H. L. Cater, K. S. Mason, M. J. Allen, A. J. Arrowood, B. D. Freeman, G. E. Sanoja and Z. A. Page, *Science*, 2022, **378**, 211–215.
39 A. Vaisman, Y. Vidavsky, M. Baranov, A. Lehrer, J. H. Baraban and N. G. Lemcoff, *J. Am. Chem. Soc.*, 2024, **146**, 73–78.
40 S. C. Leguizamon, N. T. Monk, M. T. Hochrein, E. M. Zapien, A. Yoon, J. C. Foster and L. N. Appelhans, *Macromolecules*, 2022, **55**, 8273–8282.
41 M. M. Hausladen, E. Baca, K. A. Nogales, L. N. Appelhans, B. Kaehr, C. M. Hamel and S. C. Leguizamon, *Adv. Sci.*, 2024, **11**, 2402385.
42 K. J. Stawiasz, C. I. Wendell, B. A. Suslick and J. S. Moore, *ACS Macro Lett.*, 2022, **11**, 780–784.
43 K. J. Stawiasz, J. E. Paul, K. J. Schwarz, N. R. Sottos and J. S. Moore, *ACS Macro Lett.*, 2020, **9**, 1563–1568.
44 N. Lemcoff, N. B. Nechmad, O. Eivgi, E. Yehezkel, O. Shelonchik, R. S. Phatake, D. Yesodi, A. Vaisman, A. Biswas, N. G. Lemcoff and Y. Weizmann, *Nat. Chem.*, 2023, **15**, 475–482.
45 A. E. Goetz and A. J. Boydston, *J. Am. Chem. Soc.*, 2015, **137**, 7572–7575.
46 G. Zhu, H. A. Houck, C. A. Spiegel, C. Selhuber-Unkel, Y. Hou and E. Blasco, *Adv. Funct. Mater.*, 2023, 2300456.
47 M. A. Tasdelen, *Polym. Chem.*, 2011, **2**, 2133–2145.

48 C. E. Hoyle and C. N. Bowman, *Angew. Chem., Int. Ed.*, 2010, **49**, 1540–1573.
49 S. J. Bailey, F. Stricker, E. Hopkins, M. Z. Wilson and J. Read De Alaniz, *ACS Appl. Mater. Interfaces*, 2021, **13**, 35422–35430.
50 S. J. Bailey, E. H. Discekici, E. H. Discekici, S. M. Barbon, S. N. Nguyen, C. J. Hawker, C. J. Hawker, C. J. Hawker, J. R. De Alaniz and J. R. De Alaniz, *Macromolecules*, 2020, **53**, 4917–4924.
51 A. H. St Amant, E. H. Discekici, S. J. Bailey, M. S. Zayas, J. A. Song, S. L. Shankel, S. N. Nguyen, M. W. Bates, A. Anastasaki, C. J. Hawker and J. R. De Alaniz, *J. Am. Chem. Soc.*, 2019, **141**, 13619–13624.
52 A. H. St Amant, D. Lemen, S. Florinas, S. Mao, C. Fazenbaker, H. Zhong, H. Wu, C. Gao, R. J. Christie and J. Read De Alaniz, *Bioconjugate Chem.*, 2018, **29**, 2406–2414.
53 S. J. Bailey, E. Hopkins, N. J. Baxter, I. Whitehead, J. R. de Alaniz and M. Z. Wilson, *Adv. Mater.*, 2023, **35**, 2303453.
54 S. J. Bailey, E. Hopkins, K. D. Rael, A. Hashmi, J. M. Urueña, M. Z. Wilson and J. Read de Alaniz, *Angew. Chem., Int. Ed.*, 2023, **62**, e202301157.
55 D. Ahn, L. M. Stevens, K. Zhou and Z. A. Page, *ACS Cent. Sci.*, 2020, **6**, 1555–1563.
56 D. Ahn, L. M. Stevens, K. Zhou and Z. A. Page, *Adv. Mater.*, 2021, **33**, 2104906.
57 S. N. Sanders, T. H. Schloemer, M. K. Gangishetty, D. Anderson, M. Seitz, A. O. Gallegos, R. C. Stokes and D. N. Congreve, *Nature*, 2022, **604**, 474–478.
58 D. K. Limberg, J. H. Kang and R. C. Hayward, *J. Am. Chem. Soc.*, 2022, **144**, 5226–5232.
59 C. J. O'Dea, J. Isokuortti, E. E. Comer, S. T. Roberts and Z. A. Page, *ACS Cent. Sci.*, 2024, **10**, 272–282.
60 S. Deng, J. Wu, M. D. Dickey, Q. Zhao and T. Xie, *Adv. Mater.*, 2019, **31**, 1903970.
61 M. D. Alim, K. K. Childress, N. J. Baugh, A. M. Martinez, A. Davenport, B. D. Fairbanks, M. K. McBride, B. T. Worrell, J. W. Stansbury, R. R. McLeod and C. N. Bowman, *Mater. Horiz.*, 2020, **7**, 835–842.
62 A. J. Commisso, G. R. Sama and T. F. Scott, *Chem. Mater.*, 2023, **35**, 3825–3834.
63 G. Zhu, N. von Coelln, Y. Hou, C. Vazquez-Martel, C. A. Spiegel, P. Tegeder and E. Blasco, *Adv. Mater.*, 2024, **36**, 2401561.
64 E. Goldbach, X. Allonas, L. Halbardier, C. Ley and C. Croutxé-Barghorn, *Eur. Polym. J.*, 2023, **197**, 112335.
65 T. Gonzalez Calvo, K. D. Hawkins and S. E. Seo, *J. Polym. Sci.*, 2024, **62**, 2630–2638.
66 R. D. Murphy, C. Delaney, S. Kolagatla, L. Florea, C. J. Hawker and A. Heise, *Adv. Funct. Mater.*, 2023, **33**, 2306710.
67 C. U. Lee, S. J. Kim, R. B. Dietrich, A. L. Girard and A. J. Boydston, *Green Chem.*, 2024, **26**, 9814–9822.
68 P. T. Smith, B. Narupai, J. H. Tsui, S. C. Millik, R. T. Shafranek, D. H. Kim and A. Nelson, *Biomacromolecules*, 2020, **21**, 484–492.
69 E. Sanchez-Rexach, P. T. Smith, A. Gomez-Lopez, M. Fernandez, A. L. Cortajarena, H. Sardon and A. Nelson, *ACS Appl. Mater. Interfaces*, 2021, **13**, 19193–19199.
70 V. Chiaradia, E. Pensa, T. O. Machado and A. P. Dove, *ACS Sustainable Chem. Eng.*, 2024, **12**, 6904–6912.
71 J. Guit, M. B. L. Tavares, J. Hul, C. Ye, K. Loos, J. Jager, R. Folkersma and V. S. D. Voet, *ACS Appl. Polym. Mater.*, 2020, **2**, 949–957.
72 C. Vazquez-Martel, L. Becker, W. V. Liebig, P. Elsner and E. Blasco, *ACS Sustainable Chem. Eng.*, 2021, **9**, 16840–16848.
73 N. Sadaba, E. Sanchez-Rexach, C. Waltmann, S. L. Hilburg, L. D. Pozzo, M. Olvera de la Cruz, H. Sardon, L. R. Meza and A. Nelson, *Proc. Natl. Acad. Sci. U. S. A.*, 2024, **121**, e2407929121.
74 S. Yu, N. Sadaba, E. Sanchez-Rexach, S. L. Hilburg, L. D. Pozzo, G. Altin-Yavuzarslan, L. M. Liz-Marzán, D. Jimenez de Aberasturi, H. Sardon and A. Nelson, *Adv. Funct. Mater.*, 2024, **34**, 2311209.
75 A. C. Weems, K. R. Delle Chiaie, J. C. Worch, C. J. Stubbs and A. P. Dove, *Polym. Chem.*, 2019, **10**, 5959–5966.
76 A. C. Weems, K. R. Delle Chiaie, R. Yee and A. P. Dove, *Biomacromolecules*, 2020, **21**, 163–170.
77 G. Zhu, Y. Hou, J. Xu and N. Zhao, *Adv. Funct. Mater.*, 2021, **31**, 2007173.
78 J. J. Hernandez, A. L. Dobson, B. J. Carberry, A. S. Kuenstler, P. K. Shah, K. S. Anseth, T. J. White and C. N. Bowman, *Macromolecules*, 2022, **55**, 1376–1385.
79 Z. Chen, M. Yang, M. Ji, X. Kuang, H. J. Qi and T. Wang, *Mater. Des.*, 2021, **197**, 109189.
80 T. O. Machado, C. J. Stubbs, V. Chiaradia, M. A. Alraddadi, A. Brandolese, J. C. Worch and A. P. Dove, *Nature*, 2024, **629**, 1069–1074.
81 **https://formlabs-media.formlabs.com/datasheets/2101560-TDS-ENUS-0.pdf**, (accessed 13 January 2025).
82 **https://photocentricgroup.com/wp-content/uploads/2024/09/TDS-Rigid-DL240-Plant-Based-translucent.pdf**, (accessed 13 January 2025).
83 **https://docs.carbon3d.com/files/technical-data-sheets/tds_carbon_epu-46.pdf**, (accessed 13 January 2025).
84 S. C. Gauci, P. Somers, M. Aljuaid, M. Wegener, C. Barner-Kowollik and H. A. Houck, *Adv. Funct. Mater.*, 2024, 2414713.
85 R. Rizzo, N. Petelinšek, A. Bonato and M. Zenobi-Wong, *Adv. Sci.*, 2023, **10**, 2205302.
86 A. Urciuolo, I. Poli, L. Brandolino, P. Raffa, V. Scattolini, C. Laterza, G. G. Giobbe, E. Zambaiti, G. Selmin, M. Magnussen, L. Brigo, P. De Coppi, S. Salmaso, M. Giomo and N. Elvassore, *Nat. Biomed. Eng.*, 2020, **4**, 901–915.
87 B. Huang, M. Xu and C. J. Hawker, *Macromolecules*, 2024, **57**, 4536–4543.
88 M. C. Burroughs, T. H. Schloemer, D. N. Congreve and D. J. Mai, *ACS Polym. Au*, 2023, **3**, 217–227.
89 B. T. Tuten, S. Wiedbrauk and C. Barner-Kowollik, *Prog. Polym. Sci.*, 2020, **100**, 101183.
90 A. Goyanes, U. Det-Amornrat, J. Wang, A. W. Basit and S. Gaisford, *J. Controlled Release*, 2016, **234**, 41–48.

91 J. H. Galarraga, A. P. Dhand, B. P. Enzmann and J. A. Burdick, *Biomacromolecules*, 2023, **24**, 413–425.
92 A. P. Dhand, M. A. Juarros, T. G. Martin, G. J. Rodriguez-Rivera, D. R. Hunt, M. C. Obenreder, C. O. Crosby, B. Meurer-Zeman, Q. McAfee, H. Valle-Ayala, H. M. Zlotnick, D. N. Goddard, C. C. Ebmeier, J. A. Burdick and L. A. Leinwand, *bioRxiv*, 2024, DOI: 10.1101/2024.10.01.616163.
93 G. Altin-Yavuzarslan, K. Drake, S.-F. Yuan, S. M. Brooks, E. Kwa, H. S. Alper and A. Nelson, *Matter*, 2025, **8**, 101890.
94 G. Altin-Yavuzarslan, S. M. Brooks, S.-F. Yuan, J. O. Park, H. S. Alper, A. Nelson, G. Altin-Yavuzarslan, A. Nelson, S. M. Brooks, H. S. Alper, S.-F. Yuan and J. O. Park, *Adv. Funct. Mater.*, 2023, **33**, 2300332.
95 M. R. Binelli, A. Kan, L. E. A. Rozas, G. Pisaturo, N. Prakash, A. R. Studart, M. R. Binelli, A. Kan, L. E. A. Rozas, G. Pisaturo, N. Prakash and A. R. Studart, *Adv. Mater.*, 2023, **35**, 2207483.
96 D. Dranseike, Y. Cui, A. S. Ling, F. Donat, S. Bernhard, M. Bernero, A. Areeckal, X.-H. Qin, J. S. Oakey, B. Dillenburger, A. R. Studart and M. W. Tibbitt, *bioRxiv*, 2023, 2023.12.22.572991.
97 M. Lee, R. Rizzo, F. Surman and M. Zenobi-Wong, *Chem. Rev.*, 2020, **120**, 10950–11027.
98 A. P. Dhand, M. D. Davidson, J. H. Galarraga, T. H. Qazi, R. C. Locke, R. L. Mauck and J. A. Burdick, *Adv. Mater.*, 2022, **34**, 2202261.
99 J. Guan, S. You, Y. Xiang, J. Schimelman, J. Alido, X. Ma, M. Tang and S. Chen, *Biofabrication*, 2021, **14**, 015011.
100 Y. Luo, G. Le Fer, D. Dean and M. L. Becker, *Biomacromolecules*, 2019, **20**, 1699–1708.
101 J. Kim, G. Zhang, M. Shi and Z. Suo, *Science*, 2021, **374**, 212–216.
102 A. P. Dhand, M. D. Davidson, H. M. Zlotnick, T. J. Kolibaba, J. P. Killgore and J. A. Burdick, *Science*, 2024, **385**, 566–572.
103 P. J. Scott, V. Meenakshisundaram, M. Hegde, C. R. Kasprzak, C. R. Winkler, K. D. Feller, C. B. Williams and T. E. Long, *ACS Appl. Mater. Interfaces*, 2020, **12**, 10918–10928.
104 R. H. Bean, G. Nayyar, J. I. Sintas and T. E. Long, *ACS Appl. Polym. Mater.*, 2024, **6**, 2789–2798.
105 J. Wen, R. H. Bean, G. Nayyar, K. Feller, P. J. Scott, C. B. Williams and T. E. Long, *ACS Appl. Polym. Mater.*, 2024, **6**, 2169–2176.
106 R. H. Bean, G. Nayyar, M. K. Brown, J. Wen, Y. Fu, K. I. Winey, C. B. Williams and T. E. Long, *Addit. Manuf.*, 2024, **92**, 104391.
107 J. Wen, G. Nayyar, E. R. Crater, R. H. Bean, R. Zhang, R. B. Moore and T. E. Long, *Addit. Manuf.*, 2024, **91**, 104359.
108 Z. C. Eckel, C. Zhou, J. H. Martin, A. J. Jacobsen, W. B. Carter and T. A. Schaedler, *Science*, 2016, **351**, 58–62.
109 R. Wang, C. Yuan, J. Cheng, X. He, H. Ye, B. Jian, H. Li, J. Bai and Q. Ge, *Nat. Commun.*, 2024, **15**, 1–11.
110 J. Bauer, A. Schroer, R. Schwaiger and O. Kraft, *Nat. Mater.*, 2016, **15**, 438–443.
111 J. T. Toombs, M. Luitz, C. C. Cook, S. Jenne, C. C. Li, B. E. Rapp, F. Kotz-Helmer and H. K. Taylor, *Science*, 2022, **376**, 308–312.
112 M. Li, L. Yue, A. C. Rajan, L. Yu, H. Sahu, S. M. Montgomery, R. Ramprasad and H. J. Qi, *Sci. Adv.*, 2023, **9**, eadi2958.
113 M. A. Saccone, R. A. Gallivan, K. Narita, D. W. Yee and J. R. Greer, *Nature*, 2022, **612**, 685–690.
114 J. Herzberger, V. Meenakshisundaram, C. B. Williams and T. E. Long, *ACS Macro Lett.*, 2018, **7**, 493–497.
115 K. Narita, M. A. Citrin, H. Yang, X. Xia and J. R. Greer, *Adv. Energy Mater.*, 2021, **11**, 2002637.
116 P. R. Onffroy, S. Chiovoloni, H. L. Kuo, M. A. Saccone, J. Q. Lu and J. M. DeSimone, *JACS Au*, 2024, **4**, 3706–3726.
117 D. W. Yee, M. A. Citrin, Z. W. Taylor, M. A. Saccone, V. L. Tovmasyan and J. R. Greer, *Adv. Mater. Technol.*, 2021, **6**, 2000791.
118 S. Ma, W. Bai, D. Xiong, G. Shan, Z. Zhao, W. Yi and J. Wang, *Angew. Chem., Int. Ed.*, 2024, **63**, e202405135.
119 S. Lee, P. J. Walker, S. J. Velling, A. Chen, Z. W. Taylor, C. J. B. M. Fiori, V. Gandhi, Z. G. Wang and J. R. Greer, *Nat. Commun.*, 2024, **15**, 1–11.
120 R. M. Johnson and R. A. Smaldone, *Polym. Int.*, 2025, DOI: 10.1002/PI.6713.
121 Z. Dong, H. Cui, H. Zhang, F. Wang, X. Zhan, F. Mayer, B. Nestler, M. Wegener and P. A. Levkin, *Nat. Commun.*, 2021, **12**, 1–12.
122 N. K. Mandsberg, F. Aslan, Z. Dong and P. A. Levkin, *Chem. Commun.*, 2024, **60**, 5872–5875.
123 K. S. Mason, S. Y. Huang, S. K. Emslie, Q. Zhang, S. M. Humphrey, J. L. Sessler and Z. A. Page, *J. Am. Chem. Soc.*, 2024, **146**, 4078–4086.
124 K. L. Sampson, B. Deore, A. Go, M. A. Nayak, A. Orth, M. Gallerneault, P. R. L. Malenfant and C. Paquet, *ACS Appl. Polym. Mater.*, 2021, **3**, 4304–4324.
125 P. Kunwar, A. Poudel, U. Aryal, R. Xie, Z. J. Geffert, H. Wittmann, D. Fougnier, T. H. Chiang, M. M. Maye, Z. Li and P. Soman, *Adv. Mater. Technol.*, 2024, 2400675.
126 X. Peng, L. Yue, S. Liang, S. Montgomery, C. Lu, C. M. Cheng, R. Beyah, R. R. Zhao and H. J. Qi, *Adv. Funct. Mater.*, 2022, **32**, 2112329.
127 L. Yue, S. Macrae Montgomery, X. Sun, L. Yu, Y. Song, T. Nomura, M. Tanaka and H. Jerry Qi, *Nat. Commun.*, 2023, **14**, 1–12.
128 J. J. Schwartz and A. J. Boydston, *Nat. Commun.*, 2019, **10**, 1–10.
129 K. C. H. Chin, G. Ovsepyan and A. J. Boydston, *Nat. Commun.*, 2024, **15**, 1–8.
130 K. Ehrmann and C. Barner-Kowollik, *J. Am. Chem. Soc.*, 2023, **145**, 24438–24446.
131 I. M. Irshadeen, S. L. Walden, M. Wegener, V. X. Truong, H. Frisch, J. P. Blinco and C. Barner-Kowollik, *J. Am. Chem. Soc.*, 2021, **143**, 21113–21126.
132 I. Cazin, M. O. Gleirscher, M. Fleisch, M. Berer, M. Sangermano and S. Schlögl, *Addit. Manuf.*, 2022, **57**, 102977.

133 I. Cazin, K. Plevová, W. Alabiso, E. Vidović and S. Schlögl, *Adv. Eng. Mater.*, 2024, **26**, 2301699.
134 S. L. Walden, J. A. Carroll, A. N. Unterreiner and C. Barner-Kowollik, *Adv. Sci.*, 2024, **11**, 2306014.
135 Q. Thijssen, J. A. Carroll, F. Feist, A. Beil, H. Grützmacher, M. Wegener, S. Van Vlierberghe and C. Barner-Kowollik, *Mater. Horiz.*, 2024, **11**, 6184–6191.
136 P. W. Kamm, L. L. Rodrigues, S. L. Walden, J. P. Blinco, A. N. Unterreiner and C. Barner-Kowollik, *Chem. Sci.*, 2022, **13**, 531–535.
137 T. N. Eren, F. Feist, K. Ehrmann and C. Barner-Kowollik, *Angew. Chem., Int. Ed.*, 2023, **62**, e202307535.
138 S. Bialas, L. Michalek, D. E. Marschner, T. Krappitz, M. Wegener, J. Blinco, E. Blasco, H. Frisch and C. Barner-Kowollik, *Adv. Mater.*, 2019, **31**, 1807288.
139 S. C. Gauci, M. Gernhardt, H. Frisch, H. A. Houck, J. P. Blinco, E. Blasco, B. T. Tuten and C. Barner-Kowollik, *Adv. Funct. Mater.*, 2023, **33**, 2206303.
140 F. Pashley-Johnson, R. Munaweera, S. I. Hossain, S. C. Gauci, L. Delafresnaye, H. Frisch, M. L. O'Mara, F. E. Du Prez and C. Barner-Kowollik, *Nat. Commun.*, 2024, **15**, 1–9.
141 X. Wu, K. Ehrmann, C. T. Gan, B. Leuschel, F. Pashley-Johnson, C. Barner-Kowollik, X. Wu, K. Ehrmann, F. Pashley-Johnson, C. Barner-Kowollik and C. T. Gan, *Adv. Mater.*, 2025, 2419639.
142 R. T. Michenfelder, F. Pashley-Johnson, V. Guschin, L. Delafresnaye, V. X. Truong, H. A. Wagenknecht and C. Barner-Kowollik, *Adv. Sci.*, 2024, **11**, 2402011.
143 V. X. Truong, J. Bachmann, A. N. Unterreiner, J. P. Blinco and C. Barner-Kowollik, *Angew. Chem., Int. Ed.*, 2022, **61**, e202113076.
144 M. T. Kiker, E. A. Recker, A. Uddin and Z. A. Page, *Adv. Mater.*, 2024, **36**, 2409811.
145 A. Andreu, P. C. Su, J. H. Kim, C. Siang, S. Kim, I. Kim, J. Lee, J. Noh, A. Suriya and Y. J. Yoon, *Addit. Manuf.*, 2021, **44**, 102024.
146 X. Wan, Z. Xiao, Y. Tian, M. Chen, F. Liu, D. Wang, Y. Liu, P. J. D. S. Bartolo, C. Yan, Y. Shi, R. R. Zhao, H. J. Qi and K. Zhou, *Adv. Mater.*, 2024, **36**, 2312263.
147 H. B. D. Tran, C. Vazquez-Martel, S. O. Catt, Y. Jia, M. Tsotsalas, C. A. Spiegel and E. Blasco, *Adv. Funct. Mater.*, 2024, 2315238.
148 M. M. Zieger, P. Müller, E. Blasco, C. Petit, V. Hahn, L. Michalek, H. Mutlu, M. Wegener and C. Barner-Kowollik, *Adv. Funct. Mater.*, 2018, **28**, 1801405.
149 M. Gernhardt, V. X. Truong and C. Barner-Kowollik, *Adv. Mater.*, 2022, **34**, 2203474.
150 S. C. Gauci, M. Gernhardt, H. Frisch, H. A. Houck, J. P. Blinco, E. Blasco, B. T. Tuten and C. Barner-Kowollik, *Adv. Funct. Mater.*, 2023, **33**, 2206303.
151 D. Gräfe, M. Gernhardt, J. Ren, E. Blasco, M. Wegener, M. A. Woodruff and C. Barner-Kowollik, *Adv. Funct. Mater.*, 2021, **31**, 2006998.
152 R. Batchelor, T. Messer, M. Hippler, M. Wegener, C. Barner-Kowollik and E. Blasco, *Adv. Mater.*, 2019, **31**, 1904085.
153 R. Rizzo, D. Rütsche, H. Liu, P. Chansoria, A. Wang, A. Hasenauer and M. Zenobi-Wong, *Adv. Mater. Technol.*, 2023, **8**, 2201871.
154 P. Kunwar, Z. Xiong, Y. Zhu, H. Li, A. Filip and P. Soman, *Adv. Opt. Mater.*, 2019, **7**, 1900656.
155 P. Mainik, L. Y. Hsu, C. W. Zimmer, D. Fauser, H. Steeb and E. Blasco, *Adv. Mater. Technol.*, 2023, **8**, 2300727.
156 L. Yue, X. Sun, L. Yu, M. Li, S. M. Montgomery, Y. Song, T. Nomura, M. Tanaka and H. J. Qi, *Nat. Commun.*, 2023, **14**, 1–11.
157 J. A. Herman, R. Telles, C. C. Cook, S. C. Leguizamon, J. A. Lewis, B. Kaehr, T. J. White and D. J. Roach, *Adv. Mater.*, 2024, 2414209.
158 X. Peng, X. Kuang, D. J. Roach, Y. Wang, C. M. Hamel, C. Lu and H. J. Qi, *Addit. Manuf.*, 2021, **40**, 101911.
159 S. Li, H. Bai, Z. Liu, X. Zhang, C. Huang, L. W. Wiesner, M. Silberstein and R. F. Shepherd, *Sci. Adv.*, 2021, **7**(30), eabg3677.
160 M. Tabrizi, T. H. Ware and M. R. Shankar, *ACS Appl. Mater. Interfaces*, 2019, **11**, 28236–28245.
161 L. Y. Hsu, S. G. Melo, C. Vazquez-Martel, C. A. Spiegel, F. Ziebert, U. S. Schwarz and E. Blasco, *Sci. Adv.*, 2024, **10**, 2597.
162 L. Y. Hsu, P. Mainik, A. Münchinger, S. Lindenthal, T. Spratte, A. Welle, J. Zaumseil, C. Selhuber-Unkel, M. Wegener and E. Blasco, *Adv. Mater. Technol.*, 2023, **8**, 2200801.
163 Y. Chen, J. Zhang, X. Liu, S. Wang, J. Tao, Y. Huang, W. Wu, Y. Li, K. Zhou, X. Wei, S. Chen, X. Li, X. Xu, L. Cardon, Z. Qian and M. Gou, *Sci. Adv.*, 2020, **6**(23), eaba7406.
164 X. Kuang, Q. Rong, S. Belal, T. Vu, A. M. López López, N. Wang, M. O. Arıcan, C. E. Garciamendez-Mijares, M. Chen, J. Yao and Y. S. Zhang, *Science*, 2023, **382**, 1148–1156.
165 P. Agrawal, S. Zhuang, S. Dreher, S. Mitter and D. Ahmed, *Adv. Mater.*, 2024, **36**, 2408374.
166 H. M. Zlotnick, M. M. Stevens and R. L. Mauck, *Trends Biotechnol.*, 2024, **42**, 1230–1240.
167 D. M. Wirth, C. C. Li, J. K. Pokorski, H. K. Taylor and M. Shusteff, *Addit. Manuf.*, 2024, **84**, 104081.
168 X. Zheng, W. Smith, J. Jackson, B. Moran, H. Cui, D. Chen, J. Ye, N. Fang, N. Rodriguez, T. Weisgraber and C. M. Spadaccini, *Nat. Mater.*, 2016, **15**, 1100–1106.
169 V. Hahn, P. Rietz, F. Hermann, P. Müller, C. Barner-Kowollik, T. Schlöder, W. Wenzel, E. Blasco and M. Wegener, *Nat. Photonics*, 2022, **16**, 784–791.
170 Z. J. Geffert, Z. Xiong, J. Grutzmacher, M. Wilderman, A. Mohammadi, A. Filip, Z. Li and P. Soman, *ACS Appl. Mater. Interfaces*, 2024, **16**, 69807–69817.
171 L. Stüwe, M. Geiger, F. Röllgen, T. Heinze, M. Reuter, M. Wessling, S. Hecht, J. Linkhorst, L. Stüwe, M. Geiger, F. Röllgen, T. Heinze, M. Wessling, J. Linkhorst, M. Reuter and S. Hecht, *Adv. Mater.*, 2024, **36**, 2306716.
172 K. Hsiao, B. J. Lee, T. Samuelsen, G. Lipkowitz, J. M. Kronenfeld, D. Ilyn, A. Shih, M. T. Dulay, L. Tate, E. S. G. Shaqfeh and J. M. DeSimone, *Sci. Adv.*, 2022, **8**, 2846.

173 J. M. Kronenfeld, L. Rother, M. A. Saccone, M. T. Dulay and J. M. DeSimone, *Nature*, 2024, **627**, 306–312.
174 G. Lipkowitz, T. Samuelsen, K. Hsiao, B. Lee, M. T. Dulay, I. Coates, H. Lin, W. Pan, G. Toth, L. Tate, E. S. G. Shaqfeh and J. M. DeSimone, *Sci. Adv.*, 2022, **8**, 3917.
175 Y. Pan, H. He, J. Xu and A. Feinerman, *Rapid Prototyping J.*, 2017, **23**, 353–361.
176 Y. M. Huang and C. P. Jiang, *J. Mater. Process. Technol.*, 2005, **159**, 257–264.
177 A. Khadilkar, J. Wang and R. Rai, *Int. J. Adv. Manuf. Technol.*, 2019, **102**, 2555–2569.